Results

Genetic studies

The study cohort comprised 62 unrelated Japanese LVNC probands, which included 45 sporadic cases (S) and 17 familial cases (F): a further 8 affected family members were also recruited for genotype-phenotype correlations. Table 1 summarizes the probands sex, age at diagnosis, and clinical phenotype, and the *SCN5A* variants identified.

Six heterozygous and one homozygous (rs6599230:G > A) variants were identified in 7 familial and 12 sporadic cases (Tables 1 and 2). Of these, 4 are reported in the NCBI SNP database for *SCN5A* (http://www.ncbi.nlm.nih.gov/SNP/snp_ref.cgi?geneId=6331&ctg=NT_022517.17&mrna=NM_198056.1&prot=NP_932173.1&orien=reverse), rs6599230:G > A, rs1805124:A > G (p.H558R), rs1805125: C > T (p.P1090L), and rs1805126:T > C. Two have been reported as SNPs (c.453C > T [21], c.1141-3C > A [22]). The last variant, c.3996C > T, was detected in a sporadic case of isolated LVNC with complete atrioventricular block (AVB): this variant has not been reported previously.

Association of SCN5A variants with arrhythmias

SCN5A variants were detected in 17 (50%) of the 34 probands with arrhythmias (7 familial cases and 10 sporadic cases) compared with 2 (7%) of the 28 probands without arrhythmias (Table 3): this difference was significant by Chi square analysis ($P = 0.0003$). In these 17 cases, a wide variety of arrhythmias were noted, including AVB ($n = 8$), atrial fibrillation (AF) ($n = 2$), LQTS ($n = 2$), Wolff-Parkinson-White syndrome (WPW) ($n = 5$), SSS ($n = 2$), ventricular tachycardia (VT) ($n = 7$), premature ventricular contraction (PVC) ($n = 10$), paroxysmal supraventricular tachycardia (PSVT) ($n = 3$).

While most of the variants were associated with multiple types of arrhythmia (Table 2), in the analysis of extended families multiple arrhythmia phenotypes were detected in the same family. For example for proband F6 (Fig. 2), who presented with LVNC with premature ventricular contraction (PVC), two variants were identified, rs1805126:T > C and p.P1090L. Both variants were inherited from his affected mother, who presented with LVNC with sick sinus syndrome (SSS). Using logistic regression analysis, patients who have the rs1805126:T > C variant have significantly high risk of arrhythmia (OR = 5.69 (1.05-30.84), $P = 0.044$).

We also investigated the correlation between the *SCN5A* variants and the severity of LVNC. Similar to the findings with arrhythmias, *SCN5A* variants were detected in 18 (53%) of the 34 patients who had developed heart failure, compared with just 1 (4%) of the 28 who had not. This was also a significant difference by Chi square analysis ($P = 0.0002$) (Table 4).

Discussion

During the more than ten years since mutations in the gene encoding the cardiac sodium channel, *SCN5A*, were first reported in 1995 [7], genetic alterations in *SCN5A* have been shown to influence the pathophysiology of cardiac arrhythmias, pharmacological sensitivities to antiarrhythmic drugs and recently cardiomyopathy [14]. Some common exonic SNPs were previously described as being able to produce subtle functional changes in channels physiology.

To date variations in three genes have been identified in patients with LVNC, *DTNA*, *TAZ* and *LDB3*.[4–6] Arrhythmias occur in more than 50% of patients with LVNC [23]. Since this phenotype does not correlate with the identification of gene variations, we hypothesized that variations in ion channel genes may contribute to the development of arrhythmias in LVNC patients regardless of the underlying cause of the disease. Therefore, we screened patients with LVNC for genetic variants in *SCN5A*. A significant number of genetic variations (both synonymous and non-synonymous nucleotide substitutions) were identified in the patient cohort. However, variations were detected significantly more frequently in patients who presented with arrhythmias than those who did not: 50% vs 7% ($P = 0.0003$).

Since LVNC patients with arrhythmias tend to have worse outcomes than patients without arrhythmias [23], we anticipated identifying a similar correlation between genetic variants and heart failure. Indeed *SCN5A* variants were detected in significantly more of the patients with heart failure, than this without: 53% vs 4% ($P = 0.0002$). Therefore, these data support the hypothesis that variations in ion channel encoding genes contribute to the underlying pathophysiology of LVNC and determining outcome.

The H558R substitution is located in the Na^+ channel I, II interdomain cytoplasmic linker and previous functional studies have shown that the R558-encoding minor allele can dramatically alter the phenotype of true disease-causing *SCN5A* mutations [24]. It has been suggested that it modulates Na^+ channel functional changes caused by other variations, and plays a role in intragenic complementation [25,26]. H558R expressed in the different variant backgrounds has profoundly different effectd on function, even "loss of function."[27] In our two cases with the H558R variant the QT interval was normal, but they both had severe arrhythmias, one with PVC and the other WPW. The P1090L substitution was identified in a sporadic case with AF and a familial case with PVC (proband) and SSS (the proband's mother). P1090 is localized in the II, III interdomain cytoplasmic linker. As a relatively Asian-specific common polymorphism, P1090L has been shown to result in a significant negative shift of activation midpoint in the Q1077del background [27].

With the exception of the c.3996C > T variant, all of the other variants are commonly detected in the normal popu-

Table 1
Clinical and molecular data for probands with LVNC

ID	Sex	Age	Arrhythmia	Heart failure	SCN5A variant
F1	M	0y	PVC	+	No
F2	F	69y	—	+	No
F3	M	5y	AVB	+	No
F4*	F	1w	PVC	+	c.453C > T
F5	F	60y	AVB, VT	+	RS1805126:T > C
F6	M	4y	PVC, SSS	+	RS1805126:T > C, p.P1090L
F7	F	1y	—	—	No
F8	F	5y	AF	+	RS1805126:T > C
F9	M	3m	—	+	No
F10	M	13y	LQT	+	RS6599230:G > A, RS1805126:T > C
F11	F	29y	—	+	No
F12	F	1y	—	—	No
F13	F	3y	—	—	No
F14	M	4y	—	—	No
F15	F	N/A	PVC	+	RS1805126:T > C, RS6599230:G > A
F16	F	1m	—	—	No
F17*	M	13	WPW	+	RS1805124:A > G, c.1141-3C > A
S18	F	0.2y	PSVT, WPW	+	No
S19	M	12y	PVC	+	RS1805124:A > G, c.1141-3C > A, RS1805126:T > C
S20	F	12y	AVB	+	No
S21	M	7y	AVB	+	No
S22	F	1w	WPW	+	RS1805126:T > C
S23	N/A	N/A	WPW	—	No
S24	F	21y	VT	—	No
S25	M	3y	VT	+	No
S26	M	10d	PSVT, VT	+	No
S27	M	25y	AVB	—	No
S28	M	1y	AVB	+	No
S29	F	3m	PSVT	+	RS1805126:T > C
S30	M	10y	PVC	—	No
S31	F	12y	AF	+	p.P1090L, RS1805126:T > C
S32	F	1d	LQT	—	No
S33	F	14y	VT	—	No
S34	F	1y	PVC, VT	+	No
S35	N/A	N/A	—	—	No
S36	N/A	N/A	—	+	RS1805126:T > C
S37	N/A	N/A	—	—	No
S38	N/A	N/A	—	—	No
S39	N/A	N/A	—	+	RS1805126:T > C
S40	N/A	N/A	—	—	No
S41	M	1m	—	—	No
S42	M	2m	—	+	No
S43	M	0y	AVB	+	P1332P
S44	M	9m	PVC	+	c.1141-3C > A
S45	M	3y	—	+	No
S46	M	36y	VT	+	RS1805126:T > C
S47	M	N/A	SSS	+	RS1805126:T > C
S48	F	N/A	AVB	—	No
S49	F	1y	—	—	No
S50	M	8m	WPW	—	No
S51	M	0y	—	—	No
S52	M	8m	—	—	No
S53	F	22y	—	—	No
S54	F	4m	—	+	No
S55	M	15y	—	—	No
S56	M	5m	PVC	+	RS1805126:T > C
S57	M	17y	—	—	No
S58	M	1y	—	+	No
S59	F	1y	—	—	No
S60	F	0y	—	—	No
S61	M	43y	PVC	—	RS6599230:G > A
S62	F	16y	—	—	No

F, familial case; S, sporadic case; ID indicates identification; Age, proband's age at diagnosis; N/A, information unavailable; blank, no abnormality; +, the proband had heart failure; no, no variant was found. AVB AV block; AF, atrial fibrillation; LQT, long QT syndrome; WPW, Wolff-Parkinson-White syndrome; SSS, sick sinus syndrome; VT, ventricular tachycardia; PVC, premature ventricular contraction; PSVT, paroxysmal supraventricular tachycardia.

* Compound with *LDB3* variation [6].

Table 2
Summary of *SCN5A* variants detected

DNA variant (dbSNP ID)	Protein change	Exon	Family/case	Types of arrhythmia
87G > A (rs6599230)		Exon 2	F10,F15,S61	PVC, LQT
453C > T		Exon 4	F4	PVC
1141-3C > A		Intron 9	F17, S19, S44	PVC, WPW
1673A > G (rs1805124)	H558R	Exon 12	F17, S19	PVC, WPW
3269C > T (rs1805125)	P1090L	Exon 18	F6, S31	AF, SSS, PVC
3996G > A		Exon23	S43	AVB
5457T > C (rs1805126)		Exon28	F5, F6, F8, F10, F15, S19, S22, S29, S31, S36,S39, S46, S47, S56	PSVT, VT, PVC, AVB, LQT, SSS, AF, WPW

Abbreviations are defined in Table 1.

Table 3
Incidence of *SCN5A* variants in the cases with arrhythmia and in those without arrhythmia

	SCN5A Variant			(%)	No *SCN5A* variant			(%)
	Familial cases	Sporadic cases	Total		Familial cases	Sporadic cases	Total	
Arrhythmia	7	10	17	(50)	2	15	17	(50)
No arrhythmia	0	2	2	(7)	8	18	26	(93)
Total	7	12	19	(31)	10	33	43	(69)

($P = 0.0003$).

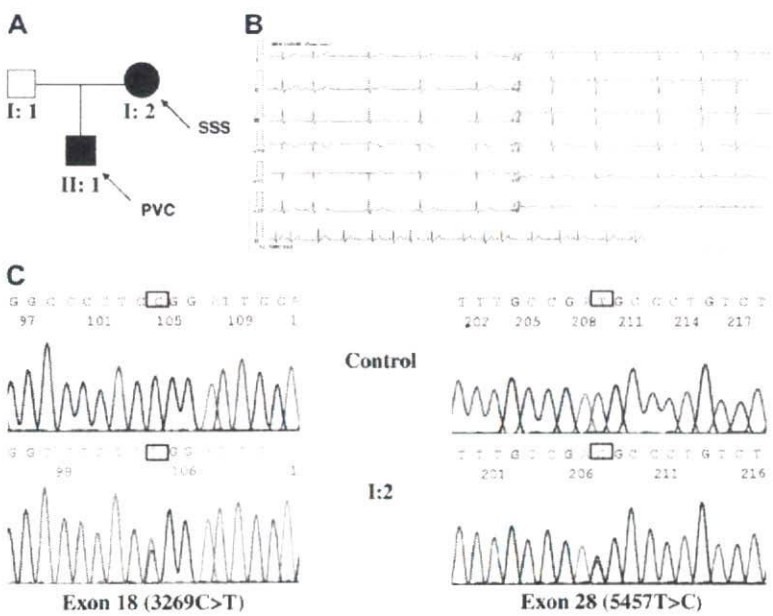

Fig. 2. (A) Pedigree of familial case 6. (B) ECG of the proband's mother who presented with SSS. (C) DNA sequence analysis of exon18 (left) and exon 28 (right) of *SCN5A* in a normal control (top) and in the proband's mother (I:2, bottom).

Table 4
Incidence of *SCN5A* variants in the cases with heart failure and in those without heart failure

	SCN5A Variant			(%)	No *SCN5A* variant			(%)
	Familial cases	Sporadic cases	Total		Familial cases	Sporadic cases	Total	
Heart failure	7	11	18	(53)	5	11	16	(47)
No heart failure	0	1	1	(4)	5	22	27	(96)
Total	7	12	19	(31)	10	33	43	(69)

($P = 0.0002$).

lation. Therefore, the question remains, how do these variants, most of which are synonymous substitutions, lead to abnormal arrhythmogenesis in the population? Regardless of their effect on the amino acid sequence, a significant number of single nucleotide substitutions alter mRNA splicing efficiency or accuracy [5]. Exonic splicing enhancer (ESE) and silencer (ESS) elements are present in most exons. Since ESEs are often distant from the canonical splice junctions, point mutations that inactivate an ESE can result in partial or complete exon skipping, affecting the structure or amounts of the expressed protein product. These splicing alterations may be incomplete, resulting in subtle changes in sodium channel expression that do not manifest changes in function in the normal heart, but in a pathological environment result in changes in cardiac repolarization, which consequently could modify the clinical expression of a latent LVNC pathogenic mutation. Rs1805126:T > C has been reported to be associated with short QTc intervals [18]. In our study, it related with the significantly high risk of the arrhythmia in LVNC patients. However, analysis using splice site prediction software (http://www.fruitfly.org/seq_tools/splice.html) or exonic splice enhancer prediction (http://genes.mit.edu/burgelab/rescue-ese/) does not predict any differences in mRNA splicing due to this SNP (data not shown).

Further, subtle changes in ion channel expression could be exacerbated by the presence of variants in proteins that interact with the ion channel. In most of the patients studied here, disease causing mutations have not been identified. Interestingly, multiple proteins containing PDZ domains have been associated with ion channel localization and function [28]. One such protein, LIM Domain Binding Protein 3 (LDB3), has been implicated in the pathogenesis of LVNC [6]. The p.D626N LDB3 variant was identified in two of the probands studied here (F4 and F17). In the first family, both the proband (F4) and her 1week old maternal twin sister carried the *LDB3* variant and the c.453C > T *SCN5A* variation. Shortly after birth, both were diagnosed with LVNC by echocardiography and have severe PVC. In the second family, the proband (F17) was initially diagnosed with isolated LVNC and WPW syndrome in a routine physical examination when he was 13 years old. He had the same variant in *LDB3*, as well as the p.H558R and c.1141-3 C > A variants in *SCN5A*. Thus it is possible to speculate that the presence of the D626N LDB3 variant, irrespective of whether it is disease-causing per se, could alter sodium channel expression, localization and/or function.

Study limitations

Due to the sensitivity of the PCR-SSCP analysis it is possible that the frequencies of SNPs reported here are lower than actually occur. However, as both patient groups were screened simultaneously without knowledge of phenotype, there would be no bias between groups for the variants identified. However, other variants may not have been detected for technical reasons and, it is possible, that they could have occurred more frequently in the groups of patients without arrhythmias. The mechanistic basis of the effect of these variants is largely unknown. Therefore, additional studies in which events such as intracellular acidosis or Ca overload can be induced may result in novel findings.

Conclusion

The prevalence of *SCN5A* variants is significantly higher in LVNC patients with arrhythmias than those without, supporting that the hypothesis that *SCN5A* variants increase arrhythmia susceptibility in LVNC. Further, the increased susceptibility to arrhythmias in turns leads to a greater risk of heart failure. We speculate that drugs targeted to the restoration of sodium channel function may offer a novel therapeutic option for patients with LVNC.

Acknowledgments

The authors thank to LVNC study collaborators: Teiji Akagi, Hikaru Doi, Hiromichi Hamada, Hidetoshi Hayakawa, Tohru Hioka, Yoshimi Hiraumi, Hitoshi Horigome, Takehiko Ishida, Shiro Ishikawa, Takamitsu Ishikawa, Hiroki Kajino, Mitsuya Kudo, Shunji Kurotobi, Tohru Matsushita, Hiroshi Mito, Toshihiro Mitomori, Masaru Miura, Toshiharu Miyake, Yasuhiro Morikami, Yasuo Murakami, Masao Nakagawa, Tomotaka Nakayama, Koichi Nihei, Masataka Nii, Yasuo Ono, Norio Sakai, Shingo Sakamoto, Hisashi Sugiyama, Mitsuo Takeda, Yasuhiko Tanaka, Hirokazu Taniguchi, Masaru Terai, Hideshi Tomita, Masaki Tsukashita, Takashi Urashima, Yasunobu Wakabayashi, Kenji Yasuda, Muneo Yoshibayashi, and Jun Yoshimoto. Fukiko Ichida is supported by grants from the Ministry of Education, Culture, Sports, Science and Technology in Japan.

References

[1] P. Richardson, W. McKenna, M. Bristow, B. Maisch, B. Mautner, J. O'Connell, E. Olsen, G. Thiene, J. Goodwin, I. Gyarfas, I. Martin and P. Nordet, Report of the 1995 World Health Organization/International Society and Federation of Cardiology Task Force on the definition and classification of cardiomyopathies, Circulation 93 (1996) 841–842.

[2] T.K. Chin, J.K. Perloff, R.G. Williams, K. Jue, R. Mohrmann, Isolated noncompaction of left ventricular myocardium: a study of eight cases, Circulation 82 (1990) 507–513.

[3] R. Engberding, F. Bender, Identification of a rare congenital anomaly of the myocardium by two-dimensional echocardiography: persistence of isolated myocardial sinusoids, Am. J. Cardiol. 53 (1984) 1733–1734.

[4] F. Ichida, S. Tsubata, K.R. Bowles, N. Haneda, K. Uese, T. Miyawaki, W.J. Dreyer, J. Messina, H. Li, N.E. Bowles, J.A. Towbin, Novel gene mutations in patients with left ventricular noncompaction or Barth syndrome, Circulation 103 (2001) 1256–1263.

[5] R. Chen, T. Tsuji, F. Ichida, K.R. Bowles, X. Yu, S. Watanabe, K. Hirono, S. Tsubata, Y. Hamamichi, J. Ohta, Y. Imai, N.E. Bowles, T. Miyawaki, J.A. Towbin, Mutation analysis of the G4.5 gene in patients with isolated left ventricular noncompaction, Mol. Genet. Metab. 77 (2002) 319–325.

[6] Y. Xing, F. Ichida, T. Matsuoka, T. Isobe, Y. Ikemoto, T. Higaki, T. Tsuji, N. Haneda, A. Kuwabara, R. Chen, T. Futatani, S. Tsubata, S. Watanabe, K. Watanabe, K. Hirono, K. Uese, T. Miyawaki, K.R. Bowles, N.E. Bowles, J.A. Towbin, Genetic analysis in patients with left ventricular noncompaction and evidence for genetic heterogeneity, Mol. Genet. Metab. 88 (2006) 71–77.

[7] Q. Wang, J. Shen, I. Splawski, D. Atkinson, Z. Li, J.L. Robinson, A.J. Moss, J.A. Towbin, M.T. Keating, SCN5A mutations associated with an inherited cardiac arrhythmia, long QT syndrome, Cell 80 (1995) 805–811.

[8] C. Bezzina, M.W. Veldkamp, M.P. van Den Berg, A.V. Postma, M.B. Rook, J.W. Viersma, I.M. van Langen, G. Tan-Sindhunata, M.T. Bink-Boelkens, A.H. van Der Hout, M.M. Mannens, A.A. Wilde, A single Na(+) channel mutation causing both long-QT and Brugada syndromes, Circ. Res. 85 (1999) 1206–1213.

[9] M. Vatta, R. Dumaine, G. Varghese, T.A. Richard, W. Shimizu, N. Aihara, K. Nademanee, R. Brugada, J. Brugada, G. Veerakul, H. Li, N.E. Bowles, P. Brugada, C. Antzelevitch, J.A. Towbin, Genetic and biophysical basis of sudden unexplained nocturnal death syndrome (SUNDS), a disease allelic to Brugada Syndrome, Hum. Mol. Genet. 11 (2002) 337–345.

[10] Q. Chen, G.E. Kirsch, D. Zhang, R. Brugada, J. Brugada, P. Brugada, D. Potenza, A. Moya, M. Borggrefe, G. Breithardt, R. Ortiz-Lopez, Z. Wang, C. Antzelevitch, R.E. O'Brien, E. Schulze-Bahr, M.T. Keating, J.A. Towbin, Q. Wang, Genetic basis and molecular mechanism for idiopathic-ventricular fibrillation, Nature 392 (1998) 293–296.

[11] D.W. Benson, D.W. Wang, M. Dyment, T.K. Knilans, F.A. Fish, M.J. Strieper, T.H. Rhodes, A.L. George, Congenital sick sinus syndrome caused by recessive mutations in the cardiac sodium channel gene (SCN5A), J. Clin. Invest. 112 (2003) 1019–1028.

[12] J.J. Schott, C. Alshinawi, F. Kyndt, V. Probst, T.M. Hoorntje, M. Hulsbeek, A.A. Wilde, D. Escande, M.M. Mannens, H. Le Marec, Cardiac conduction defects associate with mutations in SCN5A, Nat. Genet. 23 (1999) 20–21.

[13] D.W. Wang, Desai, R. Reshma, L. Crotti, M. Arnestad, R. Insolia, M. Pedrazzini, C. Ferrandi, A. Vege, T. Rognum, P.J. Schwartz, A.L. George, Cardiac sodium channel dysfunction in sudden infant death syndrome, Circulation 115 (2007) 368–376.

[14] W.P. McNair, L. Ku, M.R. Taylor, P.R. Fain, D. Dao, E. Wolfel, L. Mestroni, Familial Cardiomyopathy Registry Research Group, SCN5A mutation associated with dilated cardiomyopathy, conduction disorder, and arrhythmia, Circulation 110 (2004) 2163–2167.

[15] T.M. Olson, V.V. Michels, J.D. Ballew, S.P. Reyna, M.L. Karst, K.I. Herron, S.C. Horton, R.J. Rodeheffer, J.L. Anderson, Sodium channel mutations and susceptibility to heart failure and atrial fibrillation, JAMA 293 (2005) 447–454.

[16] M. Bienengraeber, T.M. Olson, V.A. Selivanov, E.C. Kathmann, F. O'Cochlain, F. Gao, A.B. Karger, J.D. Ballew, D.M. Hodgson, L.V. Zingman, Y. Pang, A.E. Alekseev, A. Terzic, ABCC9 mutations identified in human dilated cardiomyopathy disrupt catalytic K_{ATP} channel gating, Nat. Genet. 36 (2004) 382–387.

[17] I. Splawski, K.W. Timothy, M. Tateyama, C.E. Clancy, A. Malhotra, A.H. Beggs, F.P. Cappuccio, G.A. Sagnella, R.S. Kass, M.T. Keating, Variant of SCN5A sodium channel implicated in risk of cardiac arrhythmia, Science 297 (2002) 1333–1336.

[18] L. Gouas, V. Nicaud, M. Berthet, A. Forhan, L. Tiret, B. Balkau, P. Guicheney, D.E.S.I.R. Study Group, Association of KCNQ1, KCNE1, KCNH2 and SCN5A polymorphisms with QTc interval length in a healthy population, Eur. J. Hum. Genet. 13 (2005) 1213–1222.

[19] C.R. Bezzina, W. Shimizu, P. Yang, T.T. Koopmann, M.W. Tanck, Y. Miyamoto, S. Kamakura, D.M. Roden, A.A. Wilde, Common sodium channel promoter haplotype in asian subjects underlies variability in cardiac conduction, Circulation 113 (2006) 338–344.

[20] N. Makita, H. Tsutsui, Genetic polymorphisms and arrhythmia susceptibility, Circ. J. Suppl. A (2007) A54–A60.

[21] K. Maekawa, Y. Saito, S. Ozawa, S. Adachi-Akahane, M. Kawamoto, K. Komamura, W. Shimizu, K. Ueno, S. Kamakura, N. Kamatani, M. Kitakaze, J. Sawada, Genetic polymorphisms and haplotypes of the human cardiac sodium channel α subunit gene (SCN5A) in Japanese and their association with arrhythmia, Ann. Hum. Genet. 69 (2005) 413–428.

[22] E. Schulze-Bahr, L. Eckardt, G. Breithardt, K. Seidl, T. Wichter, C. Wolpert, M. Borggrefe, W. Haverkamp, Sodium channel gene (SCN5A) mutations in 44 index patients with Brugada syndrome: different incidences in familial and sporadic disease, Hum. Mutat. 6 (2003) 651–652. Erratum in: Hum. Mutat. 1 (2005) 61.

[23] F. Ichida, Y. Hamamichi, T. Miyawaki, Y. Ono, T. Kamiya, T. Akagi, H. Hamada, O. Hirose, T. Isobe, K. Yamada, S. Kurotobi, H. Mito, T. Miyake, Y. Murakami, T. Nishi, M. Shinohara, M. Seguchi, S. Tashiro, H. Tomimatsu, Clinical features of isolated noncompaction of the ventricular myocardium: long-term clinical course, hemodynamic properties, and genetic background, J. Am. Coll. Cardiol. 34 (1999) 233–240.

[24] T.J. Bunch, M.J. Ackerman, Promoting arrhythmia susceptibility, Circulation 113 (2006) 330–332.

[25] P.C. Viswanathan, D.W. Benson, J.R. Balser, A common SCN5A polymorphism modulates the biophysical effects of an SCN5A mutation, J. Clin. Invest. 111 (2003) 341–346.

[26] B. Ye, C.R. Valdivia1, M.J. Ackerman, J.C. Makielski, A common human SCN5A polymorphism modifies expression of an arrhythmia causing mutation, Physiol. Genomics 12 (2003) 187–193.

[27] B.H. Tan, C.R. Valdivia1, B.A. Rok, B. Ye, K.M. Ruwaldt, D.J. Tester, M.J. Ackerman, J.C. Makielski, Common human SCN5A polymorphisms have altered electrophysiology when expressed in Q1077 splice variants, Heart Rhythm 7 (2005) 741–747.

[28] O. Staub, D. Rotin, Regulation of ion transport by protein–protein interaction domains, Curr. Opin. Nephrol. Hypertens. 5 (1997) 447–454.

Circ J 2008; **72:** 1018–1019

Absence of a Trafficking Defect in R1232W/T1620M, a Double *SCN5A* Mutant Responsible for Brugada Syndrome

Naomasa Makita, MD; Naoki Mochizuki, MD*; Hiroyuki Tsutsui, MD

Background A trafficking defect of mutant cardiac Na-channels (*SCN5A*) has been implicated in Brugada syndrome. Although R1232W polymorphism and T1620M mutation by themselves have little effect on Na-channel function, their combination has been reported to disrupt membrane trafficking, resulting in a non-functioning Na channel.

Methods and Results Contrary to previous findings, patch-clamp recordings of heterologously expressed R1232W/T1620M showed robust Na currents and confocal microscopy exhibited predominant expression in the plasma membrane, similar to the wild-type channel.

Conclusions It is unlikely that an intragenic interaction between R1232W and T1620M of *SCN5A* causes a trafficking defect leading to a non-functioning Na channel. (*Circ J* 2008; **72:** 1018–1019)

Key Words: Brugada syndrome; Na channel; Trafficking defect

Brugada syndrome (BrS) is an inherited disorder of idiopathic ventricular fibrillation characterized by the ECG findings of ST elevation in the right precordial leads. Mutations in the cardiac Na channel gene (*SCN5A*) have been identified in approximately 20% of affected individuals, which commonly reveal loss-of-function properties markedly reducing Na current due to gating abnormalities[1] A defect of the membrane trafficking is another mechanism for the BrS demonstrated in several *SCN5A* mutations, including R1432G and R282H[3,4] The defect is due to retention of the protein in the endoplasmic reticulum (ER), preventing the molecule from reaching the cell surface[2]

T1620M is the first *SCN5A* mutation identified in the BrS, which exhibits gating modulation of fast inactivation and slow inactivation[5,6] However, the biophysical abnormalities produced by this mutation were relatively benign in contrast to its severe clinical phenotype. Baroudi et al reported that all the affected family members of T1620M carried a rare single nucleotide polymorphism (SNP), R1232W, on the same allele and evaluated the biophysical properties of the double mutant channel, R1232W/T1620M[7] Although R1232W and T1620M were benign by themselves, R1232W/T1620M expressed in the mammalian cells, but not in *Xenopus* oocytes, produced a non-functioning Na channel because the channel protein was retained in the ER[7-10] These findings are consistent with recent observations that *SCN5A* polymorphisms may modify phenotypic expression of disease-causing mutations. A common SNP, H558R for instance, modulates the trafficking of *SCN5A* mutations, including T512I, M1766L or R282H[4,8,9] These results suggest that the rare SNP, R1232W, may disrupt membrane trafficking of T1620M due to unknown intragenic actions[7] However, it is not clear if the trafficking defect depends upon the expression system. Thus, the present study was performed to reevaluate the biophysical properties and subcellular distribution of R1232W/T1620M using a mammalian expression system.

To avoid potential polymerase errors during mutagenesis, a small SmaI/KpnI (nt. 3115-4223) fragment of the human *SCN5A* cDNA was subcloned into pBluescript (Stratagene), and R1232W was introduced by a QuikChange site-directed mutagenesis kit (Stratagene). The entire insert was sequenced to verify the creation of the mutation and to exclude polymerase errors, and was subcloned back into the mammalian plasmid pRcCMV-T1620M to create pRcCMV-R1232W/T1620M (Fig 1A)[6] The human cell line tsA-201 (also referred to as HEK293-T) was transiently transfected with wild type (WT) or R1232W/T1620M plasmid together with a bicistronic plasmid pCD8-IRES-hβ1 encoding CD8 and the human Na-channelβ1 subunit (hβ1). Na currents were recorded using the whole-cell patch clamp technique as previously described, and multiple independent clones of each construct were evaluated[6] As shown in Fig 1B, R1232W/T1620M channels elicited robust Na current consistent with observations in *Xenopus* oocytes[10] Moreover, R1232W/T1620M was functional regardless of the coexpressed hβ1, and its gating properties, such as a positive shift of steady-state inactivation curve without changes in the activation curve demonstrated in oocytes, were confirmed in tsA-201 cells (data not shown)[10]

For the evaluation of membrane trafficking, a FLAG-tagged *SCN5A* plasmid was constructed by inserting a FLAG epitope (DYKD) in the frame right after the start codon, ATG. HEK293 cells were transiently transfected with FLAG-tagged plasmids together with pCD8-IRES-hβ1. Twenty-four hours later, cells were permeabilized with 0.05% Triton X-100, and stained with FITC conjugated

(Received February 19, 2008; revised manuscript received March 6, 2008; accepted March 16, 2008)

*Department of Cardiovascular Medicine, Hokkaido University Graduate School of Medicine, Sapporo, *Department of Structural Analysis, National Cardiovascular Center Research Institute, Suita, Japan*

Mailing address: Naomasa Makita, MD, Department of Cardiovascular Medicine, Hokkaido University Graduate School of Medicine, Kita-15, Nishi-7, Kita-ku, Sapporo 060-8638, Japan. E-mail: makitan@med.hokudai.ac.jp

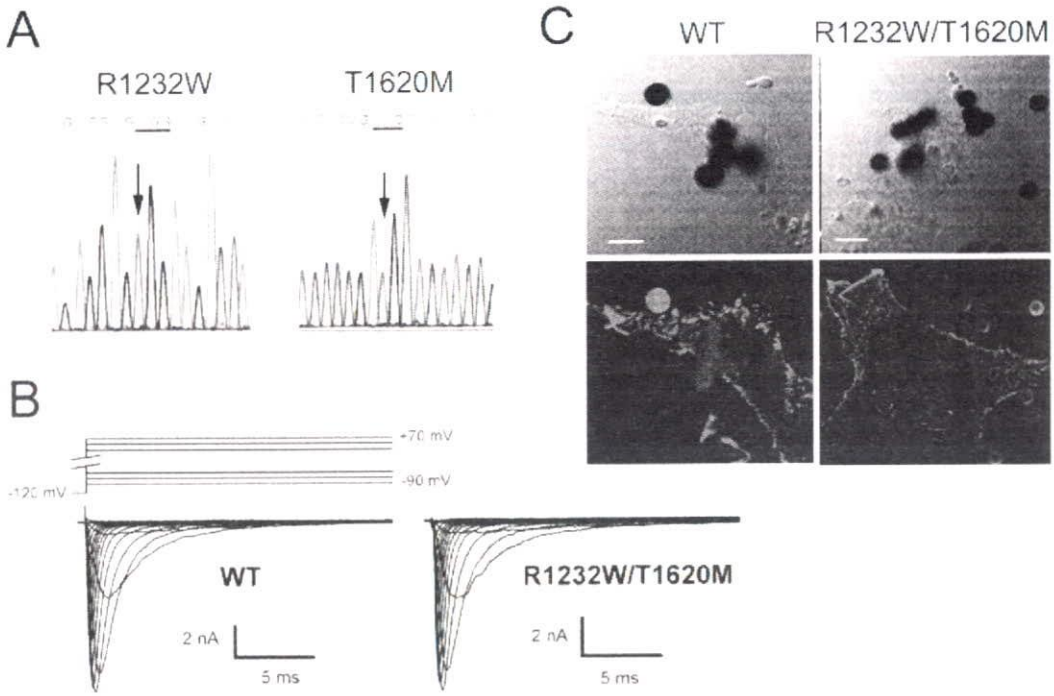

Fig 1. (A) Sequence electropherograms of R1232W (Left) and T1620M (Right) of the double mutation plasmid pRcCMV-R1232W/T1620M. Arrows indicate mutated residues. (B) Representative whole-cell Na current recordings from tsA-201 cells expressing wild type (WT) or R1232W/T1620M. Currents were recorded from a holding potential of −120 mV and stepped from −90 mV to +70 mV for 20 ms in 10 mV increments. (C) Confocal imaging of cells expressing WT and R1232W/T1620M channels. Upper and Lower panels represent differential interference contrast images and fluorescent confocal images, respectively. Fluorescent signals were predominantly detected in the plasma membrane for both the WT and R1232W/T1620M, demonstrating the absence of R1232W/T1620M trafficking abnormalities. Multiple dots are the anti-CD8 Dynabeads that identify transfected cells.

anti-FLAG M2 monoclonal antibody (Sigma-Aldrich). As shown in the fluorescence images recorded with a confocal microscope (Fig 1C), R1232W/T1620M was predominantly expressed in the plasma membrane, indistinguishable from the WT channel.

Our data clearly show that the double mutation, R1232W/T1620M, is trafficking-competent and electrophysiologically functional, consistent with findings in oocytes by Vilin et al[10] Therefore, our data do not support the earlier notion that the rare SNP, R1232W, totally disrupts the trafficking of the T1620M mutant molecule by an unknown intragenic mechanism that leads to a loss-of-function Na-channel phenotype. Unfortunately, the precise reasons for the apparent discrepancy between our data and those of Baroudi et al are not clear, but one possible explanation is unexpected sequence errors within their mutant plasmid[3]

Acknowledgements

The present study was supported in part by grants from MEXT Japan (18590757: NM), the Ministry of Health, Labour and Welfare, Japan (H18-Research on Human Genome-002: NM, and Research on Nanotechnical Medical, H19-nano-006: N. Mochizuki).

References

1. Antzelevitch C. The Brugada syndrome: Ionic basis and arrhythmia mechanisms. *J Cardiovasc Electrophysiol* 2001; **12:** 268–272.
2. Delisle BP, Anson BD, Rajamani S, January CT. Biology of cardiac arrhythmias: Ion channel protein trafficking. *Circ Res* 2004; **94:** 1418–1428.
3. Baroudi G, Pouliot V, Denjoy I, Guicheney P, Shrier A, Chahine M. Novel mechanism for Brugada syndrome: Defective surface localization of an *SCN5A* mutant (R1432G). *Circ Res* 2001; **88:** E78–E83.
4. Poelzing S, Forleo C, Samodell M, Dudash L, Sorrentino S, Anaclerio M, et al. *SCN5A* polymorphism restores trafficking of a Brugada syndrome mutation on a separate gene. *Circulation* 2006; **114:** 368–376.
5. Chen Q, Kirsch GE, Zhang D, Brugada R, Brugada J, Brugada P, et al. Genetic basis and molecular mechanism for idiopathic ventricular fibrillation. *Nature* 1998; **392:** 293–296.
6. Wang DW, Makita N, Kitabatake A, Balser JR, George AL Jr. Enhanced Na^+ channel intermediate inactivation in Brugada syndrome. *Circ Res* 2000; **87:** E37–E43.
7. Baroudi G, Acharfi S, Larouche C, Chahine M. Expression and intracellular localization of an SCN5A double mutant R1232W/T1620M implicated in Brugada syndrome. *Circ Res* 2002; **90:** E11–E16.
8. Viswanathan PC, Benson DW, Balser JR. A common SCN5A polymorphism modulates the biophysical effects of an SCN5A mutation. *J Clin Invest* 2003; **111:** 341–346.
9. Ye B, Valdivia CR, Ackerman MJ, Makielski JC. A common human SCN5A polymorphism modifies expression of an arrhythmia causing mutation. *Physiol Genomics* 2003; **12:** 187–193.
10. Vilin YY, Fujimoto E, Ruben PC. A novel mechanism associated with idiopathic ventricular fibrillation (IVF) mutations R1232W and T1620M in human cardiac sodium channels. *Pflugers Arch* 2001; **442:** 204–211.

nature genetics

Common variants in *DVWA* on chromosome 3p24.3 are associated with susceptibility to knee osteoarthritis

Yoshinari Miyamoto[1], Dongquan Shi[2], Masahiro Nakajima[1], Kouichi Ozaki[3], Akihiro Sudo[4], Akihiro Kotani[5], Atsumasa Uchida[4], Toshihiro Tanaka[3], Naoshi Fukui[6], Tatsuhiko Tsunoda[7], Atsushi Takahashi[8], Yusuke Nakamura[9], Qing Jiang[2] & Shiro Ikegawa[1]

Susceptibility to osteoarthritis, the most common human arthritis, is known to be influenced by genetic factors[1,2]. Through a genome-wide association study using ~100,000 SNPs, we have identified a previously unknown gene on chromosome 3p24.3, *DVWA*, which is associated with susceptibility to knee osteoarthritis. Expressed specifically in cartilage, *DVWA* encodes a 276-amino-acid protein with two regions corresponding to the von Willebrand factor type A domain (VWA domain)[3]. Several *DVWA* SNPs are significantly associated with knee osteoarthritis in two independent Japanese case-control cohorts. This association was replicated in a Japanese population cohort and a Han Chinese case-control cohort (combined $P = 7.3 \times 10^{-11}$). DVWA protein binds to β-tubulin, and the binding is influenced by two highly associated missense SNPs (rs11718863 and rs7639618) located in the VWA domain. The Tyr169-Cys260 isoform of DVWA, which is overrepresented in knee osteoarthritis, showed weaker interaction. Our findings reveal a new paradigm for study of osteoarthritis etiology and pathogenesis.

Osteoarthritis (MIM165720) is a common disorder that causes pain and restricted motion in joints, particularly the knee and hip[4]. About 6% of adults age 30 and older have frequent knee pain and radiographic osteoarthritis[5]. In the elderly, osteoarthritis frequently leads not only to disability but also to financial difficulty[6,7]. The critical need to manage osteoarthritis worldwide is the focus of the current 'Bone and Joint Decade' campaign. Susceptibility to osteoarthritis is influenced by genetic predisposition[8] and multiple susceptibility genes[1,2]. A few associated genes, including *FRZB*[9], *ASPN*[10] and *GDF5* (ref. 11), were identified using the candidate gene approach and confirmed in multiple populations, with functional data supporting their causality[1,12,13]. However, the genetic contribution to this complex disease is not entirely known.

The genome-wide association study is a powerful means for dissecting complex human diseases such as osteoarthritis. Susceptibility genes for several common diseases have been identified using this approach[14–16]. Notable advantages include its comprehensiveness and the potential for finding susceptibility genes with previously unknown function and relationship to the disease. As a part of the Japanese Millennium Project[14,17], we carried out a genome-wide association study for knee osteoarthritis.

To begin the study, we genotyped 94 knee osteoarthritis cases and 658 controls (set A) using 99,295 SNPs selected from the JSNP database[17]. After confirming the data quality, we compared the results of 79,763 SNPs between cases and controls by χ^2 tests for genotype, dominant, recessive and allele frequency models. We identified 2,153 SNPs that showed P values less than 0.01 in any of the four models. We further genotyped these SNPs using an independent population consisting of 646 knee osteoarthritis cases and 631 controls (set B). The SNP rs3773472 showed strong association (**Table 1**). This finding remained significant after Bonferroni correction ($0.000017 \times 2{,}153 = 0.037$). Therefore, we decided to examine SNPs around rs3773472. There were no other SNPs that showed significant association.

We referenced the International HapMap Project database (release 21a) and selected SNPs with D' value of >0.7 to rs3773472 and with a minor allele frequency of >0.1. The linkage disequilibrium (LD) block around rs3773472 contained 40 HapMap SNPs, two validated genes (*SH3BP5* and *CAPN7*) and one predicted gene (*LOC344875*). Next, we selected 12 tag SNPs (including rs3773472) that covered all 40 SNPs with an r^2 value of >0.9. After genotyping the tag SNPs using population set B, we found a more significantly associated SNP, rs7639618 ($P = 7.3 \times 10^{-8}$; **Table 2**). We examined potential

[1]Laboratory for Bone and Joint Diseases, Center for Genomic Medicine, RIKEN, 4-6-1 Shirokanedai, Minato-ku, Tokyo 108-8639, Japan. [2]The Center of Diagnosis and Treatment for Joint Disease, Drum Tower Hospital Affiliated to Medical School of Nanjing University, Zhongshan Road 321, Nanjing 210008, Jiangsu, China. [3]Laboratory for Cardiovascular Diseases, Center for Genomic Medicine, RIKEN, 1-7-22 Suehiro-cho, Tsurumi-ku, Yokohama, Kanagawa 230-0045, Japan. [4]Department of Orthopaedic Surgery, Mie University Faculty of Medicine, 2-174 Edobashi, Tsu, Mie 514-8507, Japan. [5]Department of Orthopaedic Surgery, Kyorin University, School of Medicine, 6-20-2 Shinkawa, Mitaka, Tokyo 181-8611, Japan. [6]Department of Pathomechanisms, Clinical Research Center for Rheumatology and Allergy, National Hospital Organization Sagamihara National Hospital, 18-1 Sakuradai, Sagamihara 228-8522, Japan. [7]The Laboratory for Medical Informatics, Center for Genomic Medicine, RIKEN, 1-7-22 Suehiro-cho, Tsurumi-ku, Yokohama, Kanagawa 230-0045, Japan. [8]Laboratory for Statistical Analysis, Center for Genomic Medicine, RIKEN, 4-6-1 Shirokanedai, Minato-ku, Tokyo 108-8639, Japan. [9]Laboratory for Genotyping, Center for Genomic Medicine, RIKEN, 4-6-1 Shirokanedai, Minato-ku, Tokyo 108-8639, Japan. Correspondence should be addressed to S.I. (sikegawa@ims.u-tokyo.ac.jp).

Received 27 August 2007; accepted 5 May 2008; published online 11 July 2008; doi:10.1038/ng.176

Table 1 Association of rs3773472 with knee osteoarthritis in the genome-wide analysis

	Case					Control					
	Genotype					Genotype					
Population	CC	CG	GG	Sum	Allele G frequency	CC	CG	GG	Sum	Allele G frequency	*P* value for allele frequency
Set A	52	37	5	94	0.250	259	279	77	615	0.352	0.0059
Set B	324	272	50	646	0.288	240	314	74	628	0.368	0.000017
Set A+B combined	376	309	55	740	0.283	499	593	151	1243	0.360	0.00000065

confounding factors such as age, body mass index (BMI) and sex to evaluate whether they could generate pseudo-positive associations. No significant differences in mean age, BMI and sex distribution were apparent among rs7639618 genotypes (**Supplementary Table 1** online). We also checked for a population stratification effect using a genomic control method[18,19] but found this an unlikely explanation for the positive association (**Supplementary Table 2** online).

To confirm the association, we examined an independent population cohort (set C), which was divided into knee osteoarthritis and control groups on the basis of knee radiographs. Genotyping of rs7639618 in 242 knee osteoarthritis cases and 485 controls produced another significant result (**Table 3**). We further examined the association of rs7639618 in a Han Chinese population consisting of 417 knee osteoarthritis cases and 413 controls. The association was replicated in this distinct population ($P = 0.00072$; **Table 3**), further establishing the association of the SNP. The combined P was 7.3×10^{-11} with odds ratio of 1.43 (95% CI = 1.28–1.59).

In the NCBI genome database (build 36.2), rs7639618 lies within the *LOC344875* gene. The RefSeq transcript of *LOC344875* is based on *in silico* predictions and ESTs only, so we examined the full sequence of the expressed transcript with RACE and RT-PCR. We identified a previously unknown transcript (**Supplementary Fig. 1a** online), 2,250 bp in length and with a predicted protein of 276 amino acids. Protein motif analysis programs predicted that this protein lacks a signal peptide and contains two domains homologous with the VWA domain. We named this newly identified gene *DVWA* (double von Willebrand factor A domains). Because all 17 HapMap SNPs that associated with rs7639618 with $r^2 > 0.9$ are located in and around the *DVWA* region, we surmised that *DVWA*, rather than *SH3BP5* or *CAPN7*, was likely the gene associated with osteoarthritis.

To confirm the expression and size of the *DVWA* transcript, we carried out RNA analysis and identified a band corresponding to the predicted transcript length (**Supplementary Fig. 1b**). We also examined *DVWA* expression in various human tissues using real-time PCR. The highest expression was seen in cartilage tissues from both control individuals and individuals with osteoarthritis (**Supplementary Fig. 1c**), suggesting that *DVWA* function is associated with cartilage.

To locate the functional, osteoarthritis-associated SNP, we searched for SNPs in and around all exons of *DVWA* by direct sequencing of genomic DNA from 48 individuals with knee osteoarthritis. We found 4 previously unknown SNPs in addition to 21 known SNPs in the HapMap database (**Supplementary Table 3** online). After calculating pairwise r^2 values using all 25 SNPs in the *DVWA* region (**Supplementary Fig. 2** online), we selected 7 tag SNPs with $r^2 > 0.95$. Along with the four previously genotyped SNPs, three additional SNPs (rs1287464, rs9864422 and rs11718863) were selected and genotyped. This analysis revealed that rs9864422 and rs11718863 was significantly associated with knee osteoarthritis, similar to rs7639618 (**Supplementary Table 4** online). We also checked the association of these highly associated SNPs using set C and the combined set of B and C. The association of the SNPs had similar *P* values and odds ratios in both set C and the combined set (**Supplementary Table 5** online).

Table 2 Association of the selected tag SNPs with knee osteoarthritis

	Case					Control						
	Genotype					Genotype					Test for allele frequency	
dbSNP ID	11	12	22	Sum	Allele 2 frequency	11	12	22	Sum	Allele 2 frequency	*P* value	Odds ratio (95% CI)
rs618762	515	101	8	624	0.094	536	78	7	621	0.074	0.077	0.77 (0.58–1.03)
rs7639618	253	293	95	641	0.377	162	327	140	629	0.483	0.000000073	1.54 (1.32–1.81)
rs353093	169	316	142	627	0.478	117	317	190	624	0.558	0.000062	1.38 (1.18–1.61)
rs826428	457	166	15	638	0.154	483	129	16	628	0.128	0.066	0.81 (0.65–1.01)
rs3773475	273	302	69	644	0.342	196	328	100	624	0.423	0.000024	1.41 (1.20–1.66)
rs11713836	317	266	49	632	0.288	255	291	77	623	0.357	0.00021	1.37 (1.16–1.63)
rs1318937	253	301	77	631	0.361	206	311	104	621	0.418	0.0033	1.27 (1.08–1.50)
rs3732728	349	251	43	643	0.262	287	283	59	629	0.319	0.0016	1.32 (1.11–1.56)
rs2291853	192	318	135	645	0.456	148	325	156	629	0.506	0.011	1.22 (1.05–1.43)
rs3773472	324	272	50	646	0.288	240	314	74	628	0.368	0.000017	1.44 (1.22–1.70)
rs3773469	228	315	102	645	0.402	163	336	126	625	0.470	0.00054	1.32 (1.13–1.54)
rs1287467	479	144	16	639	0.138	475	148	6	629	0.127	0.43	0.91 (0.73–1.15)

Population set B was genotyped. Allele 1 and allele 2 indicate the major and minor allele in the knee osteoarthritis population, respectively, and 11, 12 and 22 indicate homozygote of allele 1 and heterozygote and homozygote of allele 2, respectively. Odds ratio shown is for allele 1 versus allele 2.

Table 3 Replication of association of rs7639618 with knee osteoarthritis in Japanese and Han Chinese populations

	Case					Control						
	Genotype					Genotype					Test for allele frequency	
Population	GG	GA	AA	Sum	Allele A frequency	GG	GA	AA	Sum	Allele A frequency	*P* value	Odds ratio (95% CI)
Japanese (set C)	99	107	36	242	0.370	166	222	95	483	0.427	0.038	1.27 (1.01–1.59)
Chinese	145	187	85	417	0.428	106	192	115	413	0.511	0.00072	1.40 (1.15–1.69)

We analyzed haplotype association using the first tag-SNP set of 12 SNPs from the entire LD block and the second tag-SNP set of 7 SNPs in the *DVWA* region (**Supplementary Table 6** online). Using the first tag-SNP set, we could not find any haplotypes that had more significant effects than rs7639618. Also, we examined the additional effect of the other SNPs combined with the SNP (adding incrementally) by comparing their conditional log-likelihoods calculated by THESIAS[20], and confirmed that there was no SNP-combination haplotype more significant than rs7639618. Using the second tag SNP set, we found that *P* values of the difference between each haplotype and others were not more significant than those of rs9864422 and rs7639618. Also, there was no SNP-combination haplotype more significant than rs9864422 and rs7639618 . Therefore, we selected the most associated SNPs, rs9864422, rs11718863 and rs7639618, as candidates for the osteoarthritis-associated SNP for further functional analyses.

To identify a functional (causal) SNP, we first assessed the function of rs9864422, located in *DVWA* intron 1, using a luciferase assay, but there was no allelic difference associated with the SNP in the promoter or enhancer activity of *DVWA*. The two missense SNPs, rs11718863 (encoding Y169N) and rs7639618 (encoding C260Y), are in almost complete LD with each other, so it is not possible at this time to determine which one is the causal SNP, and they may act as a haplotype rather than a single SNP. The SNPs yielded three haplotypes; one haplotype (Tyr169-Cys260) was significantly over-represented in osteoarthritis (**Supplementary Table 7** online).

To evaluate their potential effects on DVWA function, we set out to identify binding partners of DVWA protein. Immunoprecipitation analysis of cells transfected with S-tagged *DVWA* revealed a unique band (**Fig. 1a**). Matrix-assisted laser desorption/ionization–time of flight (MALDI/TOF) mass spectrometry analysis revealed that this band corresponded to β-tubulin, and we confirmed binding between DVWA and β-tubulin by immunoprecipitation and protein blot analysis (**Fig. 1b**). Next, we assessed the binding strength between β-tubulin and DVWA isoforms. We generated S-tagged recombinant proteins corresponding to four haplotypes of the two missense SNPs (**Fig. 1c**) and carried out solid-phase binding assays. All four DVWA isoforms bound to tubulin, but binding of DVWA Tyr169-Cys260 was significantly weaker than that of the other three isoforms (**Fig. 1d**).

We have identified a previously unknown gene, *DVWA*, which is associated with knee osteoarthritis across two distinct Asian populations. DVWA protein is predicted to have two domains homologous to the VWA domain, which typically is involved in cell adhesion and protein–protein interactions. Mutations in the VWA domains of *MATN3* cause osteoarthritis[21] and osteochondrodysplasia[22]. Although most VWA-containing proteins are extracellular, some reside within the cell and have roles in transcription, DNA repair and ribosomal and membrane transport[23].

DVWA physically interacts with β-tubulin. The strength of binding is influenced by alleles of two missense SNPs, both of which are significantly associated with osteoarthritis and lie within the predicted VWA domain. The Tyr169-Cys260 isoform showed weaker binding to β-tubulin, whereas the other three isoforms showed similar degrees of interaction. Therefore, it seems that the binding is influenced by the two SNPs acting together rather than by one SNP alone. Because the Tyr169-Cys260 isoform is over-represented in osteoarthritis and shows weaker binding to β-tubulin, we infer that the interaction between DVWA and tubulin might protect joints from osteoarthritis. We could not identify a functional impact of rs9864422, but we do not rule out the possibility of its contribution to the susceptibility to osteoarthritis. It may influence the transcriptional activity of *DVWA* or nearby genes such as *CAPN7*.

Tubulin proteins and microtubules have essential roles in protein trafficking and secretion. Microtubules are also reported to regulate chondrocyte differentiation[24]. The addition of colchicine, an agent that depolymerizes microtubules, reduces the amount of collagen and glycosaminoglycan in chondrocytes[24]. Further, cartilage in a rat model of osteoarthritis shows a significant reduction in tubulin[25]. These

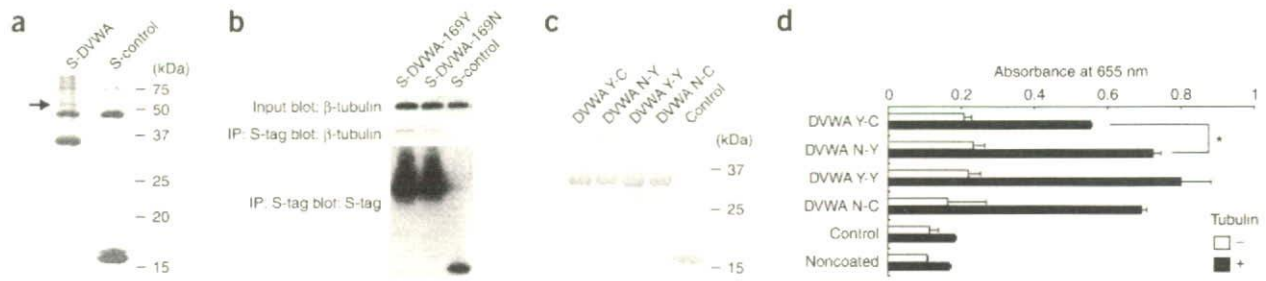

Figure 1 DVWA binds to β-tubulin. (**a**) SDS-PAGE and silver staining of samples immunoprecipitated with S-protein. Arrow indicates β-tubulin. (**b**) Confirmation of binding between DVWA and β-tubulin by protein blot. (**c**) Confirmation of DVWA recombinant proteins by SDS-PAGE. DVWA Y/N-C/Y denotes DVWA isoforms that have tyrosine (Y) or asparagine (N) at position 169, and cysteine (C) or tyrosine (Y) at position 260, respectively. (**d**) Binding strength of DVWA isoforms. Microplate wells coated with recombinant DVWA or controls were incubated with or without bovine tubulin. Data represent the mean ± s.d. in duplicate assays. The experiment was repeated three times with similar results. $^*P < 0.01$ (Student's *t*-test).

observations suggest that tubulins and microtubules might be protective factors in osteoarthritis pathogenesis. We speculate that DVWA supports intracellular transport and affects osteoarthritis susceptibility by modulating the chondrogenic function of β-tubulin. Our findings will help identify osteoarthritis pathogenesis mechanisms and aid development of improved diagnosis, treatment and prevention methods.

METHODS

Subjects. We recruited individuals with knee osteoarthritis and control individuals in sets A and B through several medical institutes in Japan, as previously described[11]. All individuals in the osteoarthritis populations were over 40 years of age. Osteoarthritis was diagnosed on the basis of clinical and radiographic findings using previously described criteria[11,26,27]. Knee osteoarthritis populations include individuals with joint-space-narrowing grade 2 or higher[26]. For set C, we recruited population-based cohorts from inhabitants of Odai and Minami-ise town (previously Miyagawa village and Nansei town, respectively[10]) in the Mie prefecture in Japan. Each subject was classified into the knee osteoarthritis or control group on the basis of radiographic findings, as previously described[10]. The Han Chinese knee osteoarthritis and control populations were recruited as described previously[11,12] from the Center for Diagnosis and Treatment of Joint Disease and the Center of Physical Examination at Drum Tower Hospital. Clinical parameters for the populations in this study are shown in **Supplementary Table 8** online. There was no significant difference in mean age, BMI and sex distribution for the genotypes of rs7639618 among the Japanese and Chinese populations studied (**Supplementary Table 1**). We obtained written informed consent from each subject as approved by the ethical committees of the SNP Research Center at RIKEN, the Medical School of Nanjing University and participating clinical institutes.

Genotyping of SNPs. We extracted genomic DNA from peripheral blood leukocytes of affected individuals and controls using standard protocols. We genotyped SNPs using the multiplex PCR–based Invader assay[28] (Third Wave Technologies) or TaqMan SNP genotyping assays (Applied Biosystems), or by direct sequencing of PCR products using ABI 3700 DNA analyzers (Applied Biosystems), according to the manufacturers' protocols. We checked the quality of genotyping data of the initial genome-wide screening and the replication study, and omitted SNPs whose genotyping success rate was lower than 90%, or whose Hardy-Weinberg equilibrium P value of the control population was lower than 0.01.

Statistical analysis. We estimated haplotype frequencies using the EM algorithm. We carried out statistical analyses for the association, haplotype frequencies and Hardy-Weinberg equilibrium and for calculation of linkage disequilibrium coefficients (D' and r^2) using Haploview software 3.32 (ref. 29) and Microsoft Excel. We selected tag SNPs using Haploview with a pairwise tagging mode. We analyzed the effect of each haplotype to the disease using THESIAS[20]. Also, we analyzed effect of SNP-combination haplotypes by adding SNPs incrementally (in a stepwise manner) and by comparing their conditional log-likelihoods calculated by THESIAS with Akaike criterion (AIC).

Cell culture and RNA extraction. We cultured HEK293, chondrogenic HCS-2/8 and OUMS-27 cells in DMEM containing 10% FBS (FBS) at 37 °C under 5% CO_2. Normal human articular chondrocytes (NHAC-kn; Cambrex) were purchased and maintained in the supplied medium of the kit. We extracted mRNA for RACE, RT-PCR and RNA blot analysis from cultured cells using the FastTrack 2.0 Kit (Invitrogen). Total RNA from cultured cells was extracted using Isogen (Nippongene) and SV Total RNA Isolation System (Promega).

We obtained knee osteoarthritis cartilage from total knee arthroplasties (7 samples). Normal cartilage was obtained from the femoral heads of control individuals during surgery for femoral neck fractures (8 samples). None of the control individuals had a clinical history or radiographic signs of osteoarthritis. We extracted total RNAs from cartilage using the RNeasy Lipid Tissue Kit (Qiagen).

RACE, RT-PCR and real-time PCR. We carried out 5′ and 3′ RACE using the SMART RACE cDNA Amplification Kit (Clontech) according to the manufacturer's protocol. We used mRNA (1 μg) of NHAC to produce the RACE template. Multiple Tissue cDNA Panels (Clontech) were used to examine all tissues other than cartilage. cDNA from cartilage and cell lines was synthesized for RT-PCR and real-time PCR using Multiscribe reverse transcriptase and an oligo-dT primer (Applied Biosystems). We carried out quantitative real-time PCR using an ABI PRISM 7700 sequence detector with the Quantitect SYBR Green PCR Kit (Qiagen) in accordance with the manufacturers' instructions.

RNA blotting. We cloned the cDNA fragment corresponding to nucleotides 510–1,517 of *DVWA* into the pCR2.1TOPO vector (Invitrogen). The DIG-labeled probe was synthesized from the constructed vector using the DIG RNA Labeling Kit (Roche). We used 4 μg of NHAC, HCS-2/8 and OUMS-27 mRNA for gel electorophoresis. Transfer, hybridization and detection were done using the DIG Easy Hyb and DIG Wash and Block Buffer set (Roche) according to the manufacturer's instructions.

Luciferase assay. We determined the core promoter region of *DVWA* and cloned a native *DVWA* promoter (nucleotide −342 to +34; the number is from the transcription start site of *DVWA*) into pGL3-basic vector (Promega), which contained the firefly luciferase gene (*Luc*). We also cloned 675-bp fragments from the genomic sequence around rs9864422 (rs9864422 fragment) that contained either allele of the SNP. Using the native *DVWA* promoter, we constructed two kinds of vectors for each allele of rs9864422 that contained the rs9864422 fragments 5′ or 3′ to the luciferase gene: (from upstream) *DVWA* promoter-rs9864422 fragment-Luc and *DVWA* promoter-Luc- rs9864422 fragment. We constructed similar vectors containing the SV40 promoter instead of the *DVWA* promoter. We transfected cells (5×10^4) with 0.4 μg of the constructed pGL3 vectors and 4 ng of the pRL-TK vector as an internal control, using TransIT-293 (for HEK293) or TransIT-LT1 (for other cell lines) reagent (Mirus). After 48 h, we collected the cells and measured luciferase activity using the PicaGene Dual Sea Pansy system (Toyo Ink).

Immunoprecipitation. The entire coding sequence of *DVWA* was cloned into the pTriEx4 vector (Novagen), which expresses N-terminal S-tagged DVWA in mammalian cells. The vector or pTriEx4 alone (which expresses S-tagged artificial control protein) was transiently transfected into HCS-2/8 or HEK293 cells. Immunoprecipitation was done on cell lysates using S-protein agarose (Novagen) according to the manufacturer's instructions. Following SDS-PAGE, target protein bands were analyzed by MALDI/TOF mass spectrometry at APRO Life Science, or by protein blotting using antibody to β-tubulin (Santa Cruz) and S-protein-HRP (Novagen).

Recombinant protein and solid-phase binding assay. Rosetta (DE3) pLacI (Novagen) was transformed with pTriEx4-*DVWA* and cultured in the Overnight Express Autoinduction System (Novagen). We extracted recombinant DVWA protein using BugBuster Protein Extraction Reagent (Novagen), and refolded it from an insoluble fraction using Protein Refolding Kit (Novagen). Maxisorp ELISA plate (Nunc) wells were coated with 100 μl of 50 μg/ml recombinant S-tagged DVWA protein in 50 mM $NaHCO_3$ buffer (pH 9.6) at 4 °C overnight. Wells were blocked with 100 μl of 5% BSA in PBS; 5 μg of bovine tubulin (Cytoskeleton) was added in a total volume of 100 μl of 5% BSA in PBS and incubated overnight at 4 °C. Wells were washed three times with 20 mM Tris-HCl (pH 7.5), 137 mM NaCl and 0.05% Tween 20 (TBST) and incubated with β-tubulin-HRP antibody (Santa Cruz) for one hour. After washing five times with TBST, we assayed bound tubulin using the TMB Peroxidase EIA Substrate Kit (Biorad).

Accession codes. DNA Data Bank of Japan: *DVWA* mRNA sequence, AB299979. GenBank: *LOC344875*, XM_497913.

Note: Supplementary information is available on the Nature Genetics website.

ACKNOWLEDGMENTS

We thank all individuals who participated in the study. We also thank S. Yamamoto, A. Fukuda, A. Kawakami, T. Kubo, Y. Takatori, S. Saito, A. Mabuchi, K. Nakamura and I. Kou for help with the research, and Y. Takanashi and T. Kusadokoro for excellent technical assistance.

AUTHOR CONTRIBUTIONS

Y.M. carried out the Japanese knee osteoarthritis association study and *in vitro* functional assay together with M.N. and prepared the manuscript. D.S. carried out the Chinese association study. K.O., A.S., A.K., A.U., N.F., Y.N. and T.Tanaka managed DNA sample and clinical information and contributed data interpretation. A.T. and T.Tsunoda helped with statistic analysis. Q.J. managed the Chinese association study. S.I. planned and supervised the whole project.

Published online at http://www.nature.com/naturegenetics/
Reprints and permissions information is available online at http://npg.nature.com/reprintsandpermissions/

1. Ikegawa, S. New gene associations in osteoarthritis: what do they provide, and where are we going? *Curr. Opin. Rheumatol.* **19**, 429–434 (2007).
2. Spector, T.D. & MacGregor, A.J. Risk factors for osteoarthritis: genetics. *Osteoarthritis Cartilage* (12 Suppl. A), S39–44 (2004).
3. Celikel, R. *et al.* Crystal structure of the von Willebrand factor A1 domain in complex with the function blocking NMC-4 Fab. *Nat. Struct. Biol.* **5**, 189–194 (1998).
4. Dieppe, P.A. & Lohmander, L.S. Pathogenesis and management of pain in osteoarthritis. *Lancet* **365**, 965–973 (2005).
5. Hunter, D.J. & Felson, D.T. Osteoarthritis. *Br. Med. J.* **332**, 639–642 (2006).
6. Pollard, B. & Johnston, M. The assessment of disability associated with osteoarthritis. *Curr. Opin. Rheumatol.* **18**, 531–536 (2006).
7. Gupta, S., Hawker, G.A., Laporte, A., Croxford, R. & Coyte, P.C. The economic burden of disabling hip and knee osteoarthritis (OA) from the perspective of individuals living with this condition. *Rheumatology (Oxford)* **44**, 1531–1537 (2005).
8. Spector, T.D., Cicuttini, F., Baker, J., Loughlin, J. & Hart, D. Genetic influences on osteoarthritis in women: a twin study. *Br. Med. J.* **312**, 940–943 (1996).
9. Loughlin, J. *et al.* Functional variants within the secreted frizzled-related protein 3 gene are associated with hip osteoarthritis in females. *Proc. Natl. Acad. Sci. USA* **101**, 9757–9762 (2004).
10. Kizawa, H. *et al.* An aspartic acid repeat polymorphism in asporin inhibits chondrogenesis and increases susceptibility to osteoarthritis. *Nat. Genet.* **37**, 138–144 (2005).
11. Miyamoto, Y. *et al.* A functional polymorphism in the 5′ UTR of GDF5 is associated with susceptibility to osteoarthritis. *Nat. Genet.* **39**, 529–533 (2007).
12. Jiang, Q. *et al.* Replication of the association of the aspartic acid repeat polymorphism in the asporin gene with knee-osteoarthritis susceptibility in Han Chinese. *J. Hum. Genet.* **51**, 1068–1072 (2006).
13. Valdes, A.M. *et al.* Sex and ethnic differences in the association of ASPN, CALM1, COL2A1, COMP, and FRZB with genetic susceptibility to osteoarthritis of the knee. *Arthritis Rheum.* **56**, 137–146 (2007).
14. Ozaki, K. *et al.* Functional SNPs in the lymphotoxin-alpha gene that are associated with susceptibility to myocardial infarction. *Nat. Genet.* **32**, 650–654 (2002).
15. Mototani, H. *et al.* A functional single nucleotide polymorphism in the core promoter region of CALM1 is associated with hip osteoarthritis in Japanese. *Hum. Mol. Genet.* **14**, 1009–1017 (2005).
16. Kubo, M. *et al.* A nonsynonymous SNP in PRKCH (protein kinase C eta) increases the risk of cerebral infarction. *Nat. Genet.* **39**, 212–217 (2007).
17. Haga, H., Yamada, R., Ohnishi, Y., Nakamura, Y. & Tanaka, T. Gene-based SNP discovery as part of the Japanese Millennium Genome Project: identification of 190,562 genetic variations in the human genome. Single-nucleotide polymorphism. *J. Hum. Genet.* **47**, 605–610 (2002).
18. Pritchard, J.K. & Rosenberg, N.A. Use of unlinked genetic markers to detect population stratification in association studies. *Am. J. Hum. Genet.* **65**, 220–228 (1999).
19. Freedman, M.L. *et al.* Assessing the impact of population stratification on genetic association studies. *Nat. Genet.* **36**, 388–393 (2004).
20. Tregouet, D.A. & Garelle, V. A new JAVA interface implementation of THESIAS: testing haplotype effects in association studies. *Bioinformatics* **23**, 1038–1039 (2007).
21. Stefansson, S.E. *et al.* Genomewide scan for hand osteoarthritis: a novel mutation in matrilin-3. *Am. J. Hum. Genet.* **72**, 1448–1459 (2003).
22. Mabuchi, A. *et al.* Novel and recurrent mutations clustered in the von Willebrand factor A domain of MATN3 in multiple epiphyseal dysplasia. *Hum. Mutat.* **24**, 439–440 (2004).
23. Whittaker, C.A. & Hynes, R.O. Distribution and evolution of von Willebrand/integrin A domains: widely dispersed domains with roles in cell adhesion and elsewhere. *Mol. Biol. Cell* **13**, 3369–3387 (2002).
24. Farquharson, C., Lester, D., Seawright, E., Jefferies, D. & Houston, B. Microtubules are potential regulators of growth-plate chondrocyte differentiation and hypertrophy. *Bone* **25**, 405–412 (1999).
25. Capin-Gutierrez, N., Talamas-Rohana, P., Gonzalez-Robles, A., Lavalle-Montalvo, C. & Kouri, J.B. Cytoskeleton disruption in chondrocytes from a rat osteoarthrosic (OA) - induced model: its potential role in OA pathogenesis. *Histol. Histopathol.* **19**, 1125–1132 (2004).
26. Ikeda, T. *et al.* Identification of sequence polymorphisms in two sulfation-related genes, PAPSS2 and SLC26A2, and an association analysis with knee osteoarthritis. *J. Hum. Genet.* **46**, 538–543 (2001).
27. Mabuchi, A. *et al.* Identification of sequence polymorphisms of the COMP (cartilage oligomeric matrix protein) gene and association study in osteoarthrosis of the knee and hip joints. *J. Hum. Genet.* **46**, 456–462 (2001).
28. Ohnishi, Y. *et al.* A high-throughput SNP typing system for genome-wide association studies. *J. Hum. Genet.* **46**, 471–477 (2001).
29. Barrett, J.C., Fry, B., Maller, J. & Daly, M.J. Haploview: analysis and visualization of LD and haplotype maps. *Bioinformatics* **21**, 263–265 (2005).

Biochemical and Biophysical Research Communications 378 (2009) 589–594

Contents lists available at ScienceDirect

Biochemical and Biophysical Research Communications

journal homepage: www.elsevier.com/locate/ybbrc

Evaluation of channel function after alteration of amino acid residues at the pore center of KCNQ1 channel

Taruna Ikrar [a,b], Haruo Hanawa [a], Hiroshi Watanabe [a], Yoshiyasu Aizawa [a,*], Mahmoud M. Ramadan [a], Masaomi Chinushi [a], Minoru Horie [c], Yoshifusa Aizawa [a]

[a] Division of Cardiology, First Department of Internal Medicine, Niigata University Graduate School of Medical and Dental Sciences, 1-754 Asahimachi Dori, Chuo-ku, Niigata 951-8510, Japan
[b] The National Agency for Drug and Food Control, Republic of Indonesia, Jakarta, Indonesia
[c] Department of Cardiovascular and Respiratory Medicine, Shiga University of Medical Science, Shiga, Japan

ARTICLE INFO

Article history:
Received 17 November 2008
Available online 3 December 2008

Keywords:
Long QT syndrome
Missense mutation
KCNQ1
I_{Ks}
Pore center
Amino acid residue

ABSTRACT

The effect of the electrical charge or the size of the amino acid residue at the pore center of a slowly activation component of the delayed rectifier potassium channel: KCNQ1 was studied. K^+ currents were measured after transfection of one of four KCNQ1 mutants: substituting Isoleucine with Lysine, Glutamate, Valine or Glycine and then transfected in COS-7 cells. Both the negatively- and positive charged residue I313 K and I313E showed a loss of function when expressed alone and a dominant negative suppression when co-expressed with wild type KCNQ1. When the site was substituted with the smallest neutral amino acid residue: I313G, there was a small reduction of current when transfected alone and a gain of function when co-transfected with the wild type. I313V showed no difference from the wild type. Changes of amino acid residue at the pore center of KCNQ1 may alter the channel function but this depends on the electrical charge or the size of amino acid residue.

The delayed rectifier K^+ current (I_{Ks}) channel is formed by the co-assembly of KCNQ1 (KvLQT1) with KCNE1 (minK) and contributes to repolarizing cardiac myocytes [1]. A mutation in either subunit is well known to cause long QT syndrome (LQTS) which predisposes affected individuals to cardiac arrhythmias and sudden death [2,3].

In LQTS, the phenotype was suggested to be affected by the site of the mutation and patients with trans-membrane mutations had more frequent diagnostic criteria, LQTS-related cardiac events and a prolonged QT-interval after exercise than patients with a C-terminal mutation [4]. However, this finding from Japan is in contrast to that of the International Long QT Syndrome Registry in which the phenotypes were not related to the site of the mutation [5].

We have previously characterized the physiological consequences of the LQTS-associated mutation at the pore center: I313K, in a patient with a severe LQT1 phenotype [6]. The mutant channels showed almost no current when transfected alone but when co-expressed with WT-KCNQ1, they showed a dominant negative suppression [6].

In this report, our aim was to explore the effects of the charge and the size of the amino acid residue at the pore center of KCNQ1. In order to do this, we substituted its Isoleucine residue with electrically charged ones: Lysine and Glutamate and two neutral amino acids: Valine and Glycine, and performed an electrophysiological study after transfection of each mutant.

Materials and methods

Construction of plasmid DNA for gene transfer. A full-length human WT-KCNQ1, KCNE1, and mutant KCNQ1 were inserted into a plasmid vector pIRES2-EGFP using BamHI restriction sites making the pIRES2-EGFP-KCNQ1, pIRES-EGFP-KCNE1, and mutant pIRES2-EGFP-I313K plasmids as described previously [6]. In the pIRES2-EGFP-I313K plasmid, we introduced three new missense mutations which can occur in humans. One is a mutant with Glutamate which is a positively charged large amino acid residue (I313E). Then we prepared two mutants, Valine (I313V), a neutral amino acid of similar size and homology to the Isoleucine residue in WT-KCNQ1 [7–10] and Glycine as the smallest sized neutral amino acid (I313G).

The mutation of I313E was introduced with a PCR reaction using the mutant primer sets: 5′-GTGGTCACAGTCACCACC*gaa*GGCTATGGGGACAAGGTG-3′ and 5′-CACCTTGTCCCCATAGCC*ttc*GGTGGTGACTGTGACCAC-3′ (*lower case letters indicate mutation sites*). The mutation of I313V was introduced with a PCR using the mutant primer sets 5′-GTGGTCACAGTCACCACC*gtc*GGCTATGGGGACAAGGTG-3′ and 5′-CACCTTGTCCCCATAGCC*gac*GGTGGTGACTGTGACCAC-3. For the mutation of I313G, we used the primer sets 5′-GTGGTCACAGTCACCA

* Corresponding author. Fax: +81 25 228 5611.
E-mail address: aizaways@med.niigata-u.ac.jp (Y. Aizawa).

0006-291X/$ - see front matter © 2008 Elsevier Inc. All rights reserved.
doi:10.1016/j.bbrc.2008.11.076

CC*ggc*GGCTATGGGGACAAGGTG-3′ and 5′-CACCTTGTCCCCATAGC C*gcc*GGTGGTGACTGTGACCAC-3′.

For these experiments, we used the QuickChange site-directed mutagenesis kit (Stratagene, La Jolla, CA, USA). The resulting products were again amplified by PCR using the primers 5′-CCATTTCCATC ATCGACCTCA-3′ and 5′-AAGGAGAGCGCTGGTGAAG-3′. This final PCR product was ligated to the pIRES2-EGFP WT-KCNQ1 vector using the PstI sites at nucleotide positions 697 and 1675 of KCNQ1. The PCR insert was also cleaved with PstI prior to ligation. The resulting four cloned plasmids were then transformed into *Escherichia coli* JM109 competent cells and purified using a Quantum Prep Plasmid Maxi prep kit (Bio-Rad Laboratories, Hercules, CA).

Culture and transfection of COS-7 cells. A COS-7 monkey kidney cell line was obtained from the American Type Cell Collection and cultured in Dulbecco's modified Eagles medium (Invitrogen Corporation, Gibco-BRL, Rockville, MD) supplemented with 1% penicillin–streptomycin (prepared with 10,000 U/ml penicillin G sodium and 10,000 μg/ml streptomycin sulfate in 0.85% saline) and 10% fetal bovine serum in a humidified 5% CO_2 incubator at 37 °C. The number of cells seeded per ml of medium was 2×10^5 on average. Cultured cells were seeded in 60 mm plates 24 h before transfection, then transiently transfected with various plasmids by the Fugene-6 method (Roche Applied Science, Indianapolis, IN).

Electrophysiological experiments. The whole-cell patch-clamp method was applied to COS-7 cells transfected with the wild type and/or mutant plasmids as described previously [6,11,12]. Briefly, cells were allowed to settle at the bottom of a bath (0.5 ml) mounted on an inverted microscope (Olympus Corp., Tokyo, Japan). Cells were superfused with the bath solution (140 mmol NaCl, 5.4 mmol KCl, 0.5 mmol $MgCl_2$, 1.8 mmol $CaCl_2$, 0.33 mmol NaH_2PO_4, 5.5 mmol glucose and 5 mmol HEPES) and the pH was adjusted to 7.4 by using NaOH. When inserted into the cell/bath solution, a glass pipette with an internal diameter of 1.0–1.5 μm had a resistance of 4–6 MΩ when filled with the following internal solution: 100 mmol/l K-aspartate, 20 mmol/l KCl, 5 mmol/l ATP-Mg, 5 mmol/l phosphocreatine-dipotassium, 5 mmol/l EGTA, 5 mmol/l HEPES and 1 mmol/l $CaCl_2$ (the pH was adjusted to 7.2 with KOH). A patch-clamp amplifier Axopatch 200B (Axon Instruments, Foster City, CA) was used to record membrane currents.

After obtaining a whole-cell configuration, cell membrane capacitance was estimated by analyzing the transient capacitance elicited by 5 mV hyperpolarizing pulses. Cells were held at a starting potential of −80 mV and depolarizing pulses of various potentials ranging from −80 to +80 mV in 20 mV increments for 2 s were applied, followed by repolarization to −40 mV for 2 s to record tail currents. The pCLAMP 8.0 software (Axon Instruments, Foster City, CA) was used to generate the pulse protocol, data acquisition, and analyses.

To be confident of the currents obtained, our analyses only included recordings obtained by Giga-seal after applying the following quality control criteria for the patch-clamp technique [13]: (1) the starting seal resistance was required to be more than 1 GΩ, (2) the series resistance was required to be lower than 20 MΩ throughout the recording, (3) the membrane potential was required to be at a higher negative level than −50 mV if normal high-potassium intracellular solution was used; and (4) cell capacitance and resistance were required to be stable. Furthermore, to check the quality of our findings, COS-7 cells transfected with wild type KCNQ1 were compared with the results of Barhanin et al. [1] and Sanguinetti et al. [15] regarding the properties and biophysical characteristics of the wild type KCNQ1 potassium current.

Data analyses. Analyses of the data were performed with Clampfit 9.1 (Axon Instruments, Foster City, CA) and SPSS for Windows ver.15 (SPSS Inc., Chicago, IL). The time constants for activation and deactivation were determined by fitting the current recordings with a single-exponential function [16]: $f(t) = A_0 + A\,exp(-t/\tau)$ and the voltage dependence of channel activation and deactivation were fitted with the Boltzmann equation: $I = I_{max}/(1 + exp[(V_{1/2} - V)/k])$, where A was current amplitude, τ was the time constant, t was time, I was current amplitude, I_{max} was the maximal tail current, V was the test pulse potential, $V_{1/2}$ was the half-maximal activation potential, and k was the slope of the activation curve. The relationship of current density with side-chain residue volume was measured after 2 s during depolarization.

Results for continuous normal data were expressed as mean ± standard error of estimation. The comparison of means of continuous normal variables across a grouping variable with two levels was done using the student's t-test and the comparison of means of continuous normal variables across a grouping variable with several levels was undertaken with one-way analysis of variance (ANOVA). A two-sided significance level of 0.05 was used for all analyses.

Results

Wild type and mutant channel currents

The cells transfected with KCNQ1 and KCNE1 exhibited a slowly activated outward current compatible with I_{Ks} from native cardiac myocytes. Each mutant was then transfected with KCNE1 and the current–voltage relationships of the peak current during depolarization and the tail current were measured as Fig. 1.

I313 G ($n = 17$ cells) showed an approximately 20% reduction in peak current and the densities of the peak and tail currents were less than those of the wild type ($n = 10$ cells) but the differences were not significant ($P = 0.987$). The activation curve shifted towards the left (Fig. 1A, B, F and Table 1). I313V ($n = 15$ cells) exhibited no significant change in the current compared to those of the wild type ($P = 1.00$, Fig. 1A–C and F). The shape of the membrane potential vs. the current density curve was also similar among cells transfected with the wild type and I313V ($P = 1.00$, Fig. 1F and G).

I313K ($n = 14$ cells) produced almost no current and I313E ($n = 15$ cells) showed a marked reduction of current compared to the wild type ($P < 0.01$ for both, Fig. 1A, D, E and Table 1).

Co-expression of WT and mutant KCNQ1 channels

Cells were then co-transfected with 0.5 μg of each mutant and 0.5 μg of the wild type together with KCNE1 (Fig. 2). Co-transfection of I313 G with the wild type ($n = 16$ cells) showed a 2-fold increase of the current compared to the cells transfected with the wild type: 110.7 ± 4.7 vs. 57.1 ± 6.2 pA/pF ($P < 0.001$) (Fig. 2A and B) and the tail current was also significantly augmented: 26.2 ± 1.7 vs. 16.0 ± 2.3 pA/pF ($P < 0.05$). The activation curve was shifted towards the left (Fig. 2E and F). I313 V co-transfected with the wild type ($n = 9$ cells) showed similar current intensities without significant differences ($P = 1.00$) compared to the wild type ($n = 11$ cells) (Fig. 2A, C and Table 1). Co-transfection of I313E with the wild type ($n = 15$ cells) exhibited a similar current to that of cells co-transfected with I313 K and the wild type ($n = 14$ cells) both showing >70% reduction of current amplitude compared to the wild type ($P < 0.001$) (Fig. 2D–E, and Table 1). An increased current in I313G with the wild type suggested a gain of function and a markedly reduced current in I313E and I313K when co-expressed with the wild type would reflect a dominant negative suppression (Fig. 2F–G).

Kinetic analysis of mutant KCNQ1 channels

The hetero-tetrameric of the wild type and mutant channel in the presence of KCNE1 showed peak and tail currents which were well fitted with the Boltzmann equation or a single-exponential

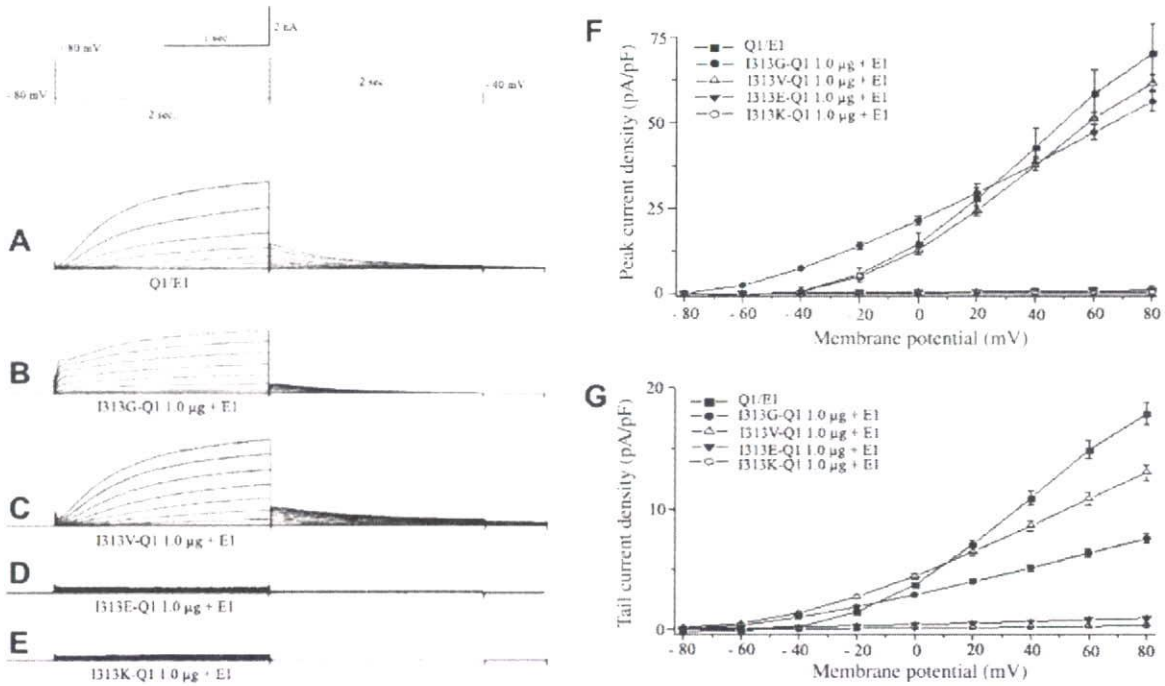

Fig. 1. Results of the whole-cell patch-clamp experiments in COS-7 cells. COS-7 cells were transfected with plasmids of wild type KCNQ1 (Q1) and four mutants together with (E1)KCNE1 (A–E). The activation is rapid but the peak current was about 20% smaller in I313G (B) compared with the wild type (A). I313K and I313E showed almost no current (D,E). The current–voltage relationships of cells transfected with five plasmids are shown on the right and a shift to the left can be seen in I313G (F). The differences in the peak and tail currents among the wild type and four mutants were not significant. Pulse protocol and graph scale are shown at the top.

Table 1
Comparison of kinetics and peak currents in COS-7 cells transfected with wild type and/or mutant KCNQ1 plasmids.

Plasmid DNA	Peak current	Activation curve (mV)		Time constants (τ, ms)	
	(pA/pF)	(V1/2)	Slope (*k*)	Activation	Deactivation
WT 1.0 ng (*n* = 10)	70.4 ± 8.7 2	17.0 ± 1.4	17.0 ± 1.4	1252.0 ± 14.2	2.0 ± 14.2220
I313G 1.0 ng (*n* = 17)	56.4 ± 2.7[†]	17.6 ± 1.3[‡]	19.9 ± 1.2[†]	607.4 ± 5.2[‡]	397.2 ± 14.5[†]
I313V 1.0 ng (*n* = 15)	61.8 ± 2.2[†]	20.9 ± 1.6[†]	17.3 ± 1.1[†]	1389.6 ± 5.7[†]	369.3 ± 110.6[†]
I313E 1.0 ng (*n* = 15)	0.9 ± 1.1[‡]	–	–	–	–
I313K 1.0 ng (*n* = 14)	0.4 ± 0.2[‡]	–	–	–	–
WT[#] (*n* = 11)	57.1 ± 6.2	23.2 ± 1.3	16.7 ± 1.1	1154.3 ± 62.8	213.6 ± 11.85
WT/I313G (*n* = 16)	110.7 ± 4.7[*]	15.6 ± 1.2[*]	20.2 ± 1.3[*]	350.8 ± 3.0[*]	648.4 ± 126.0[*]
WT/I313V (*n* = 9)	59.5 ± 1.5[§]	22.5 ± 1.1[§]	16.9 ± 1.0[§]	1297.5 ± 5.7[§]	327.53 ± 110.6[§]
WT/I313E (*n* = 15)	9.3 ± 0.5[*]	19.0 ± 1.1[§]	18.1 ± 1.0[§]	1242.2 ± 91.4[§]	289.0 ± 74.4[§]
WT/I313K (*n* = 14)	14.6 ± 1.7[*]	23.9 ± 1.8[§]	17.1 ± 1.6[§]	1302.1 ± 88.2[§]	388.4 ± 64.4[§]

Data represents the mean ± SEM.
WT, wild type; KCNQ1 (α subunit of the potassium voltage-gated channel KQT-like subfamily member 1); KCNE1, β subunit of the potassium voltage-gated channel I_{Ks}-related family member 1; I313K;I313E;I313V and I313G: mutant KCNQ1.
[‡] $P < 0.01$ vs. WT 1.0 μg/KCNE1 1.0 μg.
[†] $P > 0.05$ vs. WT 1.0 μg/KCNE1 1.0 μg.
[#] 0.5 μg of WT was transfected and subsequent study was transfected 0.5 μg of mutant.
[*] $P < 0.001$ vs. WT 0.5 μg/KCNE1 1.0 μg.
[§] $P > 0.05$ vs. WT 0.5 μg/KCNE1 1.0 μg. Each plasmid was transfected with KCNE1 (see text).

function [16]. The activation curves for cells transfected with the wild type and that of co-transfection with I313K, I313E or I313V were not significantly different (Table 1).

Expression of I313G alone showed a more rapid initial activation compared to the wild type: 607.4 ± 5.2 vs. 1252.0 ± 14.2 ms ($P < 0.01$) and smaller $V_{1/2}$: 17.6 ± 1.3 vs. 23.5 ± 1.4 mV ($P < 0.01$) as shown in Fig. 1 and Table 1. I313 G co-transfected with the wild type showed a significant shift in the activation curve towards the left compared with the wild type and the time constant of activation was smaller: 350.8 ± 3.0 vs. 1154.3 ± 62.8 ms ($P < 0.001$) while that of deactivation of the tail current was larger: 648.4 ± 126.0 vs. 213.6 ± 11.85 ms ($P < 0.001$) as shown in Fig. 2A and B, Table 1).

The activation curves for cells transfected with I313E, I313K and I313V together with the wild type revealed statistically non-significant differences compared to cells transfected with the wild type alone ($P = 0.99$, Fig. 2). The time constants were similar among these three mutants but that of I313G was larger at the membrane potential<−25 mV and smaller at >−25 mV (Fig. 3A).

The current density was also affected by the side-chain volume of amino acid residue at position 313 and a significantly larger current density was found only when I313G was co-expressed with the wild type compared with when it was expressed alone (Fig. 3B). Both the homo-tetrameric and hetero-tetrameric I313G

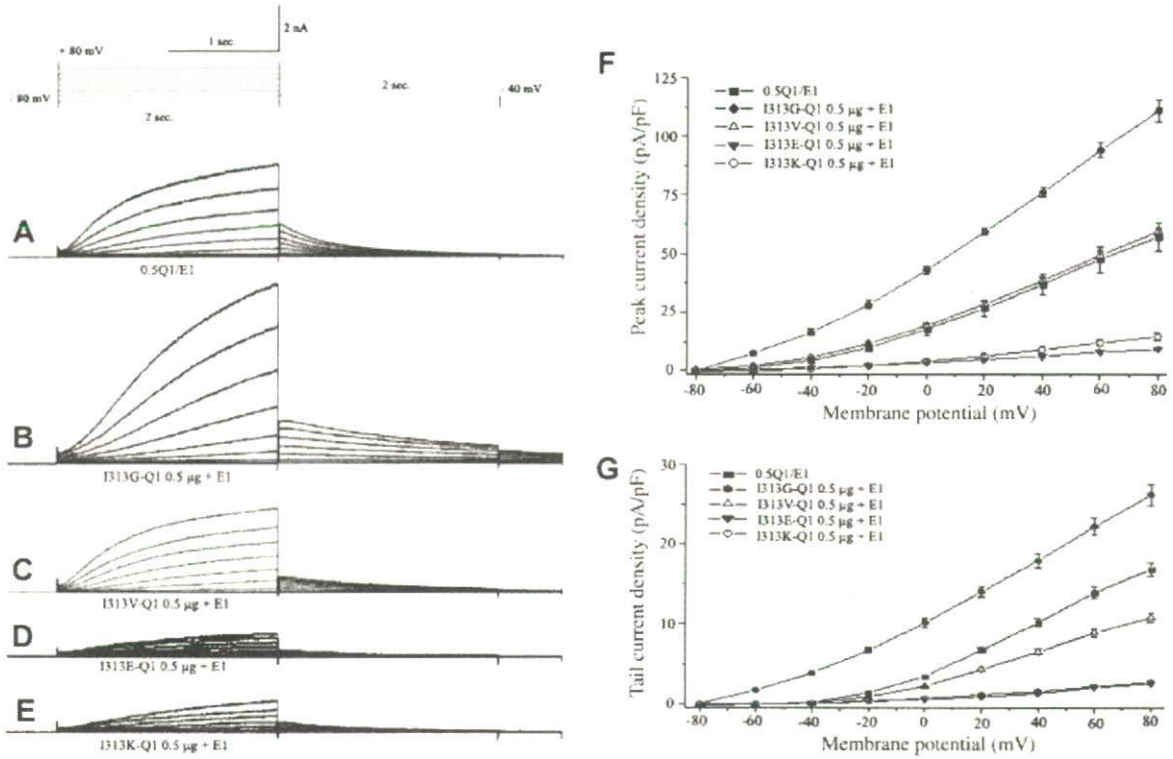

Fig. 2. Results of the whole-cell patch-clamp experiments in COS-7 cells. COS-7 cells were co-transfected with wild type KCNQ1 and four mutants together with KCNE1 (A–E). Current–voltage relationships are shown on the right (F,G). Augmented peak ($P < 0.001$) and tail current ($P < 0.05$) and a shift to the left in activation curve was observed when I313G was co-transfected with the wild type KCNQ1 (B and F). Dominant negative suppression was seen in D and E in which the amino acid residue was replaced by an either positive or negative charged one (D,E). Pulse protocol and graph scale are shown at the top.

with the wild type showed a shift to the left in the activation curve (Fig. 3C) suggesting a altered gating.

Discussion

Both negatively charged (I313K) and positively charged (I313E) residues at the pore center of KCNQ1 resulted in an apparent loss of channel function when they were transfected alone (with KCNE1). The loss of function was not due to a trafficking defect and when they were co-transfected with wild type KCNQ1 (with KCNE1), a dominant negative suppression was observed.

The I_{Ks} channel has six trans-membrane domains (S1–S6), a voltage sensor (S4) and a pore helix selectivity filter segment (P-loop) that connects S5 and S6 [10,17]. The selectivity filter is reflected in a highly conserved amino acid sequence for specific ion conductance as elegantly defined by the crystal structure of the bacterial KcsA channel [18] and the carbonyl oxygen atoms of these residues which bind dehydrated K^+ ions and act for selectivity [19,20]. An altered charge at the pore center, I313K and I313E, is expected to result in a crucial change of the electrostatic environment of the selectivity filter, with serious consequences that reduce the conduction of K^+ ions [21–24]. The presence of charged amino acid residues at the pore center may also disturb the closed/open equilibrium and lead to the destabilization of the open-state of the channel [25] but this was not confirmed in the present study.

The current density was also affected by the side-chain volume of the amino acid residue at the pore center (Fig. 3B and Table 1). When we substituted the neutral Isoleucine residue of KCNQ1 with Valine (I313V) which has a similar size and polarity to Isoleucine, the normalized current–voltage relationship was very similar to the wild type. The homo-tetramer of the Glycine residue (I313G) showed a reduction of the peak K^+ current by about 20% compared with the wild type, but the initial current was larger (Fig. 1B). Furthermore when I313G was co-expressed with the wild type KCNQ1, the K^+ current increased 2-fold which suggests a gain of function (Fig. 2B).

The conductive conformation of the K^+ channel represents a match between the ion-binding sites and the size of K^+ ions [26] and the filter atoms and the surrounding protein atoms are important for selective ion-binding and conduction [9,10]. The volume of side-chain residues located in position 313 may affect conduction of K^+ ions [27].

For the augmented K^+ currents observed in the I313G mutant, we postulate as follows. The homo-tetramer by the smallest amino acid residue Glycine minimized the selectivity filter size (pore) and resulted in a reduced peak current. However, when the mutant was co-transfected with the wild type, the pore was composed of mixed amino acid residue, Glycine and Isoleucine rendered the channel pore larger and augmented the K^+ current (Fig. 3C). Using Brownian dynamics on a simplified model of the KcsA structure, it was shown that altering the pore size of the cytosolic entrance to the selectivity filter led to a change in conductance [28].

As limitations, except for I313K, other mutants are virtual and we have no clinical counterparts so far, but if I313G is associated with short QT syndrome or not is of interest [29]. The change in ion selectivity in each mutant and the relation to the gating mechanism was not fully studied in the present report [30].

As clinical implications, the functional consequences of mutations at the pore center of KCNQ1 varied: from dominant negative suppression to a gain of function when co-transfected with wild type KCNQ1. Severe reduction of I_{Ks} would be detectable as LQTS but a subtle change in K^+ channel function of varying degrees might go undetected.

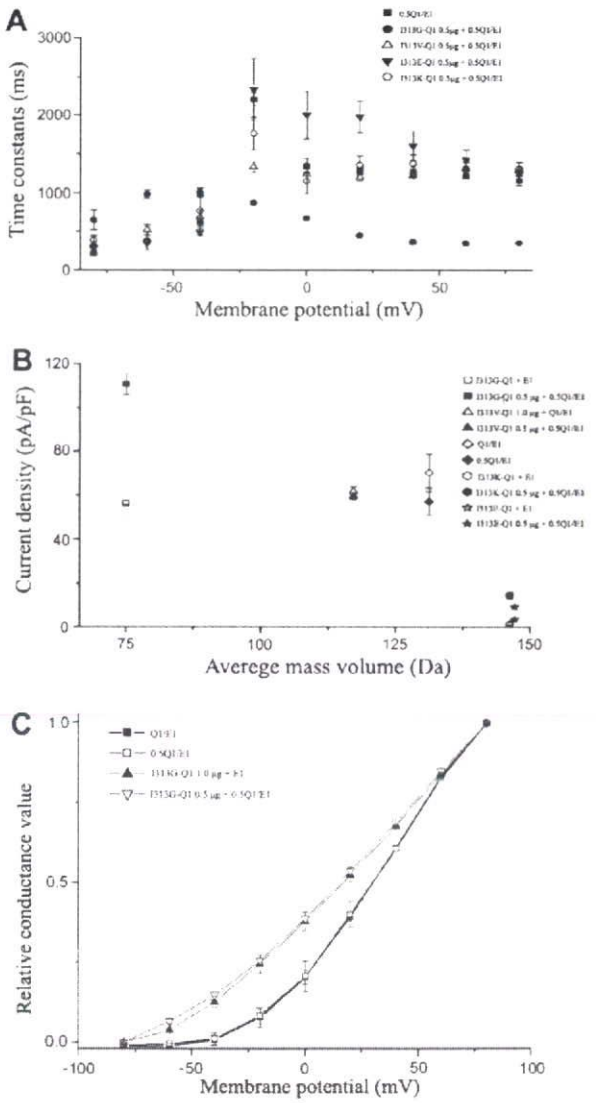

Fig. 3. Activation and deactivation kinetics of currents in the wild type and mutant K^+ channels. In A, activation and deactivation kinetics of co-expression mutants and the wild type KCNQ1 together with KCNE1 are shown. The time constants were derived from the raw current traces and plotted as the function of membrane potential. Substitution of amino acid residue at the pore center (313) altered the relation between the time constant and membrane potential. In B, currents measured at +80 mV and were plotted against the side-chain mass average volume of the residues at position 313 ($n = 9–19$). The current was least in I313K and I313E but larger when I313G was co-expressed with the wild type. I313V was close to the wild type. In C, relative conductance of the initial tail current amplitude was similar when I313G was transfected alone or with the wild type (+KCNE1). Both shifted toward the left compared to the wild type.

In conclusion, charged residues at the pore center of KCNQ1 resulted in a loss of K^+ channel function and a dominant negative pattern when co-transfected with the wild type channel. The neutral residues showed zero or a small reduction of the K^+ current and some mutants might show a gain of function when co-expressed with the wilt type channel. Not only the site of the mutation but the alteration in charge or size seems to affect phenotype of LQTS.

Acknowledgment

This work was supported by a grant from the Japanese Ministry of Education, Science and Culture, Tokyo, Japan.

References

[1] J. Barhanin, F. Lesage, E. Guillemare, M. Fink, M. Lazdunski, G. Romey, K(V)LQT1 and IsK (minK) proteins associate to form the I(Ks) cardiac potassium current, Nature 384 (1996) 78–80.
[2] A.J. Moss, R.S. Kass, Long QT syndrome: from channels to cardiac arrhythmias, J. Clin. Invest. 115 (2005) 2018–2024.
[3] E. Marban, Cardiac channelopathies, Nature 415 (2002) 213–218.
[4] W. Shimizu, M. Horie, S. Ohno, K. Takenaka, M. Yamaguchi, M. Shimizu, T. Washizuka, Y. Aizawa, K. Nakamura, T. Ohe, T. Aiba, Y. Miyamoto, Y. Yoshimasa, J.A. Towbin, S.G. Priori, S. Kamakura, Mutation site-specific differences in arrhythmic risk and sensitivity to sympathetic stimulation in the LQT1 form of congenital long QT syndrome: multicenter study in Japan, J. Am. Coll. Cardiol. 44 (2004) 117–125.
[5] W. Zareba, J.A. Moss, G. Sheu, E.S. Kaufman, S. Priori, G.M. Vincent, J.A. Towbin, J. Benhorin, P.J. Svhwartz, C. Napolitano, W.J. Hall, M.T. Keating, M. Qi, J.L. Robinsdon, M.L. Andrews, International LQTS registry. Location of mutation in the KCNQ1 and phenotypic presentation of long QT syndrome, J. Cardiovasc. Electrophysiol. 14 (2003) 1149–1153.
[6] T. Ikrar, H. Hanawa, H. Watanabe, S. Okada, Y. Aizawa, M.M. Ramadan, S. Komura, F.Y. amashita, M. Chinushi, Y. Aizawa, A double point mutation in the selectivity filter site of the KCNQ1 potassium channel results in a severe phenotype, LQT1, of long QT syndrome, J. Cardiovasc. Electrophysiol. 19 (2008) 541–549.
[7] D.J. Snyders, Structure and function of cardiac potassium channels, Cardiovasc. Res. 42 (1999) 377–390.
[8] D.M. Roden, Defective ion channel function in the long QT syndrome: multiple unexpected mechanisms, J. Mol. Cell. Cardiol. 33 (2001) 185–187.
[9] S. Berneche, B. Roux, A gate in the selectivity filter of potassium channels, Structure 13 (2005) 591–600.
[10] D.A. Doyle, J.M. Cabral, R.A. Pfuetzner, A. Kuo, J.M. Gulbis, S.L. Cohen, B.T. Chait, R. MacKinnon, The structure of the potassium channel: molecular basis of K^+ conduction and selectivity, Science 280 (1998) 69–77.
[11] Y. Aizawa, K. Ueda, F. Scornik, J.M. Cordeiro, Y. Wu, M. Desai, A. Guerchicoff, Y. Nagata, Y. Iesaka, A. Kimura, M. Hiraoka, C. Antzelevitch, A novel mutation in KCNQ1 associated with a potent dominant negative effect as the basis for the LQT1 form of the long QT syndrome, J. Cardiovasc. Electrophysiol. 18 (2007) 972–977.
[12] Y. Hosaka, H. Nanawa, T. Washizuka, M. Chinushi, F. Yamashita, T. Yoshia, S. Komura, H. Watanabe, Y. Aizawa, Function, subcellular localization and assembly of a novel mutation of KCNJ2 in Andersen's syndrome, J. Mol. Cell. Cardiol. 35 (4) (2003) 409–415. Apr.
[13] A. Molleman, Patch Clamping: An Introductory Guide to Patch Clamp Electrophysiology, John Wiley & Sons, England, 2003. pp. 107–108..
[15] M.C. Sanguinetti, M.E. Curran, A. Zou, J. Shen, P.S. Spector, D.L. Atkinson, M.T. Keating, Coassembly of K(V)LQT1 and minK (IsK) proteins to form cardiac I(Ks) potassium channel, Nature 384 (1996) 80–83.
[16] I.R. Boulet, A.L. Raes, N. Ottschytsch, D.J. Snyders, Functional effects of a KCNQ1 mutation associated with the long QT syndrome, Cardiovasc. Res. 70 (2006) 466–474.
[17] G. Seebohm, N. Strutz-Seebohm, O.N. Ureche, R . Baltaev, A. Lampert, G. Kornichuk, K. Kamiya, T.V. Wuttke, H. Lerche, M.C. Sanguinetti, F. Lang, Differential roles of S6 domain hinges in the gating of KCNQ potassium channels, Biophys. J. 90 (2006) 2235–2244.
[18] A.D. Wei, A. Butler, L. Salkoff, KCNQ-like potassium channels in *Caenorhabditis elegans* conserved properties and modulation, J. Biol. Chem. 280 (2005) 21337–21345.
[19] J.A. Smith, C.G. Vanoye, A.L. George Jr., J. Meiler, C.R. Sanders, Structural models for the KCNQ1 voltage-gated potassium channel, Biochemistry 46 (2007) 14141–14152.
[20] T.W. Allen, A. Bliznyuk, A.P. Rendell, S.H. Kuyucak, The potassium channel: structure, selectivity and diffusion, J. Chem. Phys. 112 (2000) 8191–8204.
[21] J. Aqvist, V. Luzhkov, Ion permeation mechanism of the potassium channel, Nature 404 (2000) 881–884.
[22] S.Y. Noskov, S. Bernèche, B. Roux, Control of ion selectivity in potassium channels by electrostatic and dynamic properties of carbonyl ligands, Nature 431 (2004) 830–834.
[23] Y. Zhou, R. MacKinnon, The occupancy of ions in the K^+ selectivity filter: charge balance and coupling of ion binding to a protein conformational change underlie high conduction rates, J. Mol. Biol. 333 (2003) 965–975.
[24] D. Bichet, M. Grabe, Y.N. Jan, L.Y. Jan, Electrostatic interactions in the channel cavity as an important determinant of potassium channel selectivity, Proc. Natl. Acad. Sci. USA 103 (2006) 14355–14360.
[25] G. Seebohm, P. Westenskow, F. Lang, M.C. Sanguinetti, Mutation of colocalized residues of the pore helix and transmembrane segments S5 and S6 disrupt deactivation and modify inactivation of KCNQ1 K^+ channels, J. Physiol. 563 (2005) 359–368.
[26] S.W. Lockless, M. Zhou, R. MacKinnon, Structural and thermodynamic properties of selective ion binding in a K+ channel, PLoS Biol. 121 (2007) 1079–1088.
[27] L.J. Mullins, An analysis of pore size in excitable membranes, J. Gen. Physiol. 43 (1960) 105–117.
[28] S.H. Chung, T.W. Allen, S. Kuyucak, Conducting-state properties of the KcsA potassium channel from molecular and Brownian dynamics simulations, Biophys. J. 82 (2002) 628–645.

[29] C. Bellocq, A.C. Ginneken, C.R. Bezzina, M. Alders, D. Escande, M.M. Mannens, I. Baró, A.A. Wilde, Mutation in the KCNQ1 gene leading to the short QT-interval syndrome, Circulation 109 (2004) 2394–2397.

[30] T. Lu, A.Y. Ting, J. Mainland, L.Y. Jan, P.G. Schultz, J. Yang, Probing ion permeation and gating in a K^+ channel with backbone mutations in the selectivity filter, Nat. Neurosci. 4 (2001) 239–246.

nature genetics

SNPs in *BRAP* associated with risk of myocardial infarction in Asian populations

Kouichi Ozaki[1], Hiroshi Sato[2], Katsumi Inoue[3], Tatsuhiko Tsunoda[4], Yasuhiko Sakata[2], Hiroya Mizuno[2], Tsung-Hsien Lin[5,6], Yoshinari Miyamoto[7], Asako Aoki[1], Yoshihiro Onouchi[1], Sheng-Hsiung Sheu[5,6], Shiro Ikegawa[7], Keita Odashiro[3], Masakiyo Nobuyoshi[3], Suh-Hang H Juo[8–10], Masatsugu Hori[2], Yusuke Nakamura[11] & Toshihiro Tanaka[1]

Myocardial infarction is a common disease and among the leading causes of death in the world. We previously reported association of variants in *LGALS2*, encoding galectin-2, with myocardial infarction susceptibility in a case-control association study in a Japanese population[1]. Here we identify BRAP (BRCA1-associated protein) as a galectin-2–binding protein. We report an association of SNPs in *BRAP* with myocardial infarction risk in a large Japanese cohort ($P = 3.0 \times 10^{-18}$, OR = 1.48, 2,475 cases and 2,778 controls), with replication in additional Japanese and Taiwanese cohorts ($P = 4.4 \times 10^{-6}$, 862 cases and 1,113 controls and $P = 4.7 \times 10^{-3}$, 349 cases and 994 controls, respectively). BRAP expression was observed in smooth muscle cells (SMCs) and macrophages in human atherosclerotic lesions. *BRAP* knockdown by siRNA using cultured coronary endothelial cells suppressed activation of NF-κB, a central mediator of inflammation.

We previously reported a genome-wide association study for myocardial infarction[1], in which we found an association between myocardial infarction susceptibility and SNPs in *LTA*, encoding a cytokine produced in an early stage of the vascular inflammatory process. We identified galectin-2 protein as a binding partner of LTA protein[2], and we also identified a functional SNP in *LGALS2* (encoding galectin-2) that affected LTA secretion and that was also associated with risk of myocardial infarction in the Japanese population[2]. Replication studies have been done for these associations in populations of other ancestries[3–6]. To further understand the molecular mechanism that confers risk of myocardial infarction, we searched for proteins that interact with galectin-2. By means of tandem affinity purification[7], followed by matrix-assisted laser desorption/ionization–time of flight (MALDI/TOF) mass spectrometry analyses, we identified BRAP, BRCA1-associated protein, as a possible binding partner of galectin-2 (**Fig. 1a**). Tubulin protein, previously reported as a binding partner of galectin-2 (ref. 2), was also detected (**Fig. 1a**). We examined the interaction between BRAP and galectin-2 in COS7 cells using constructs designed to express Myc-tagged galectin-2 or S-tagged BRAP and protein blot analysis, and confirmed their interaction by coimmunoprecipitation experiments (**Fig. 1b**).

To examine whether genetic variation in *BRAP* is associated with susceptibility to myocardial infarction, we searched for SNPs in a 47-kb genomic region of *BRAP* by resequencing genomic DNAs from 24 Japanese individuals and identified a total of 50 SNPs (**Supplementary Table 1** online). Twenty-six of them were previously unknown, according to searches in the dbSNP database (as of the end of April 2008, Build 129; **Supplementary Table 1**). Genotyping

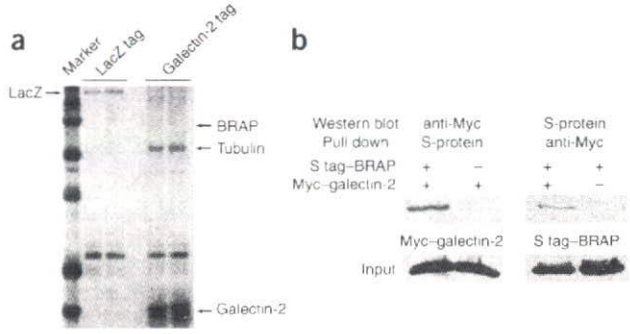

Figure 1 Galectin-2 interacts with BRAP. (**a**) Isolation of TAP-tagged galectin-2 and interacting proteins. (**b**) Coimmunoprecipitation of Myc-tagged galectin-2 and S-tagged BRAP in COS7 cells.

[1]Laboratory for Cardiovascular Diseases, Center for Genomic Medicine, RIKEN, Yokohama 230-0045, Japan. [2]Department of Cardiovascular Medicine, Osaka University Graduate School of Medicine, Osaka 565-0871, Japan. [3]Department of Cardiology, Kokura Memorial Hospital, Kitakyushu 802-8555, Japan. [4]Laboratory for Medical Informatics, Center for Genomic Medicine, RIKEN, Yokohama 230-0045, Japan. [5]Division of Cardiology, Department of Internal Medicine, Kaohsiung Medical University Hospital, Kaohsiung 807, Taiwan. [6]Department of Internal Medicine, Kaohsiung Medical University, Kaohsiung 807, Taiwan. [7]Laboratory for Bone and Joint Disease, Center for Genomic Medicine, RIKEN, Tokyo 108-8639, Japan. [8]Department of Medical Research, Kaohsiung Medical University Hospital, Kaohsiung 807, Taiwan. [9]Graduate Institute of Medical Genetics, Kaohsiung Medical University, Kaohsiung 807, Taiwan. [10]Center of Excellence for Environmental Medicine, Kaohsiung Medical University, Kaohsiung 807, Taiwan. [11]Center for Genomic Medicine, RIKEN, Yokohama 230-0045, Japan. Correspondence should be addressed to T.T. (toshitan@src.riken.jp).

Received 1 July 2008; accepted 20 November 2008; published online 8 February 2009; doi:10.1038/ng.326

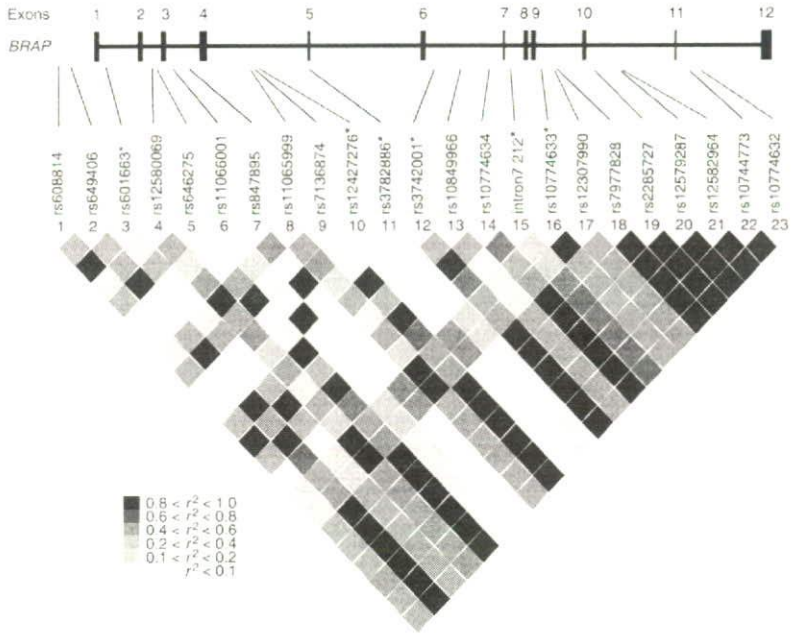

Figure 2 LD map of *BRAP* locus. Asterisks (*) indicate six tag SNPs.

these 50 SNPs in approximately 100 myocardial infarction cases and 100 control individuals showed that 23 SNPs had minor allele frequencies (MAF) greater than 5% (**Supplementary Table 1**). We selected six tag SNPs from these 23 SNPs with pairwise tagging only and r^2 threshold of 0.8 using Haploview software[8] (**Fig. 2** and **Supplementary Table 2** online). We compared genotype frequencies of these tag SNPs in about 450 individuals with myocardial infarction and 450 controls and found that one SNP, rs3782886, in exon 5 (90A>G, R241R) of *BRAP* was significantly associated with myocardial infarction ($P = 0.0014$, comparison of allele frequency, **Supplementary Table 3** online). Haplotypes based on these six tag SNPs showed a less significant association with myocardial infarction than rs3782886 (**Supplementary Table 4** online). To further examine the effect of these haplotypes, we applied THESIAS[9] and observed a significant effect on disease susceptibility between the most and second-most frequent haplotypes that could be distinguished by rs3782886 alone. Consideration of the conditional log-likelihoods with Akaike information criterion (AIC) indicated that rs3782886 had a smaller AIC value than the haplotype model, so we concluded that rs3782886 alone rather than the haplotypes explained an association with myocardial infarction. We also applied a logistic regression analysis to search for combinatorial effects of other SNPs to rs3782886, but did not find any that were significant (**Supplementary Table 5** online). These results suggest that rs3782886 or other SNPs with high linkage disequilibrium (LD) to rs3782886 may be the causative variants.

rs11066001 was in very strong LD ($r^2 = 0.96$) with rs3782886, so we examined these two SNPs in 2,475 cases and 2,778 controls, and found strong associations with myocardial infarction ($\chi^2 = 83.6$, $P = 3.0 \times 10^{-18}$, OR = 1.48, by comparison of allele frequency of rs11066001, **Table 1**). To further confirm the association, we examined two additional panels, 862 cases and 1,113 controls from the Japanese population and 349 cases and 994 controls from the Taiwanese population, and confirmed the associations of rs11066001 and rs3782886 with myocardial infarction in these two sets (**Table 1**).

According to HapMap data[10], minor allele frequencies of rs3782886 were 0.239 in Japanese in Tokyo and 0.148 in Han Chinese in Beijing, but this allele was observed in neither CEPH individuals (Utah residents with ancestry from northern and western Europe) nor Yoruba individuals from Ibadan, Nigeria. No information was available for rs11066001. We additionally examined a panel of 50 CEPH individuals and found that there was no variation at these two SNP loci (data not shown). These results indicate that these SNPs are likely to be present only in Asian populations. However, the possibility cannot be excluded that other variations in this gene confer risk of myocardial infarction in other populations. In the WTCCC study[11], six SNPs in the *BRAP* region were examined, and the lowest *P* value among these SNPs was 0.0013 at rs601663. This does not meet the genome-wide significance threshold for this study, leaving open the question of association in other populations.

Because rs1041981 in *LTA* and rs7291467 in *LGALS2* were associated with myocardial infarction as reported in our previous study[1,2], we also carried out logistic regression analysis[12] for the combinatorial effect of rs11066001 (*BRAP*), rs1041981 (*LTA*) and rs7291467 (*LGALS2*) on myocardial infarction susceptibility. We did not find any evidence of gene–gene interactions, as addition of a statistical interaction term showed no significance (see Methods). The combinatorial effect was consistent with a multiplicative-odds-ratio model.

Table 1 Association of the two *BRAP* SNPs (rs11066001 and rs3782886) with myocardial infarction

	rs11066001				rs3782886			
	MAF				MAF			
Study population	Cases	Controls	OR (95% CI)	*P* value	Cases	Controls	OR (95% CI)	*P* value
Japanese								
First panel	0.34	0.26	1.48 (1.36–1.61)	3.0×10^{-18}	0.35	0.28	1.42 (1.31–1.54)	2.8×10^{-15}
Replication panel	0.34	0.26	1.46 (1.27–1.67)	4.4×10^{-6}	0.36	0.27	1.50 (1.31–1.71)	1.8×10^{-7}
Combined	0.34	0.26	1.47 (1.37–1.56)	1.3×10^{-24}	0.35	0.27	1.44 (1.34–1.55)	7.0×10^{-23}
Taiwanese	0.33	0.27	1.31 (1.09–1.58)	4.7×10^{-3}	0.33	0.28	1.26 (1.05–1.52)	1.5×10^{-2}

P values adjusted for Bonferroni's correction in both Japanese cohorts.